GLOBAL BIOGEOCHEMICAL CYCLES, VOL. 12, NO. 2, PAGES 277–295, JUNE 1998

# Long-term variability of the terrestrial and oceanic carbon sinks and the budgets of the carbon isotopes $^{13}C$ and $^{14}C$

Fortunat Joos and Michele Bruno
Physics Institute, University of Bern, Bern, Switzerland

**Abstract.** The long-term variability in the terrestrial and oceanic uptake of anthropogenic carbon is investigated. Ice core and direct observations of atmospheric $CO_2$ and $^{13}C$ are used for the last 200 years. An inverse method called double deconvolution is applied. It is found that the biosphere turned from a carbon source of about 0.5 Gt C $yr^{-1}$ into a sink of 1 Gt C $yr^{-1}$ during the first half of this century. This is in qualitative agreement with earlier reconstructions based on atmosperic $CO_2$ data and implies a terrestrial sink to compensate land use emissions during the last five decades. Oceanic and biospheric carbon uptakes are estimated to be 0.9±1.0 and 1.1±1.0 Gt C $yr^{-1}$ as averaged over the 1970-1990 period. Hence ocean uptake is on the low side of current estimates, but our results may be biased as $\delta^{13}C$ observations between 1956 and 1982 are missing. Additional uncertainties in calculated carbon sinks are due to uncertainties in model parameters and in fossil emission estimates. Prior to 1950, uncertainties are primarily related to uncertainties in the ice core $\delta^{13}C$ data; a Monte Carlo analysis yields a 1-$\sigma$ uncertainty in the terrestrial and oceanic uptake of ±0.36 Gt C $yr^{-1}$ when ice core data are smoothed over a 50 year period. The budget of bomb-produced radiocarbon is reinvestigated. We could not find model solutions that concomitantly match the bomb budget and the observed atmospheric $\delta^{13}C$ and prebomb $\Delta^{14}C$ decrease. The closure of the budget would require a relatively low oceanic and biospheric $^{14}C$ uptake that conflicts with the relatively high isotopic uptake rates required to simulate the observed decrease in $\delta^{13}C$ and $\Delta^{14}C$. We conclude that recent estimates of bomb test productions and/or the stratospheric $^{14}C$ decrease are not compatible with published $^{13}C$ and $^{14}C$ observations.

## 1. Introduction

An understanding of the mechanisms that govern the uptake of anthropogenic $CO_2$ by the ocean and biosphere is required to link future carbon emissions, atmospheric $CO_2$, and associated climate changes. Carbon sources and sinks vary on different time scales and space scales. The reconstruction of these variations using observed data would provide an independent test for models used to simulate future atmospheric $CO_2$ concentrations. However, a reconstruction of the long-term variability of the anthropogenic carbon uptake by ocean and land biosphere is missing. Here we use observations of atmospheric $CO_2$ and $^{13}C$ as well as $^{14}C$ to reconstruct the oceanic and biospheric net sink (or source) fluxes and their decadal to centennial variability for the past 200 years.



Paper number 98GB00746.
0886-6236/98/98GB-00746$12.00

The classical method to estimate terrestrial and oceanic carbon storage for the industrial period is by solving the budget for atmospheric $CO_2$. The method by which this is done is referred to as a "single deconvolution" [*Siegenthaler and Oeschger*, 1987]. In the single deconvolution, oceanic uptake is calculated by an ocean transport model. Then, the terrestrial sink flux is estimated as the difference between the change in observed atmospheric plus modeled oceanic carbon inventory and fossil emission. Such analyses find that the terrestrial biosphere acted as a net carbon source of the order of 0.5 Gt C $yr^{-1}$ before 1933 and as a net sink of about 0.3 Gt C $yr^{-1}$ after 1943 [*Bruno and Joos*, 1997]. This implies an average biospheric carbon sink of 1.5 Gt C $yr^{-1}$ during the last five decades to compensate for estimated carbon emissions by land use changes [*Houghton*, 1993] and to close the budget of anthropogenic $CO_2$.

The addition of atmospheric $^{13}C$ observations permits one to estimate carbon fluxes using an inverse method referred to as a "double deconvolution." Combined observations of $CO_2$ and the carbon isotope $^{13}C$ have been used by two groups to quantify short-term

interannual fluctuations of the air-sea and air-biota exchange fluxes for the last decade [*Keeling et al.*, 1989a, 1995; *Francey et al.*, 1995]. The double deconvolution technique and related analyses have also been applied to estimate local air-sea and air-terrestrial fluxes using observations of the latitudinal gradients of $CO_2$ and $^{13}C$ [e.g., *Pearman and Hyson*, 1986; *Keeling et al.*, 1989a; *Ciais et al.*, 1995; *Enting et al.*, 1995]. *Heimann and Maier-Reimer* [1996] have recently summarized three other methods [*Quay et al.*, 1992; *Tans et al.*, 1993] to determine the average oceanic and biospheric carbon uptake from $^{13}C$ observations. They estimate an average oceanic uptake rate of 2.1± 0.9 Gt C $yr^{-1}$ for the 1970-1990 period.

In this paper, we use a double deconvolution technique to reconstruct the magnitude of the oceanic and terrestrial carbon sinks for the last 200 years. In such a double deconvolution, atmospheric $CO_2$ and $^{13}C$, fossil carbon, and $^{13}C$ emissions are prescribed from observations. Then, the atmospheric budget equations for the two tracers are solved for the unknown sink fluxes. Carbon exchange fluxes between atmosphere, ocean, and biosphere result in a net transfer of $^{13}C$ when the reservoirs are in isotopic disequilibrium even when no net carbon transfer is involved. These disequilibrium fluxes are important terms in the $^{13}C$ budget and thus crucial in order to estimate the net terrestrial and oceanic carbon storage. Here we employ models for the ocean [*Siegenthaler and Joos*, 1992; *Joos et al.*, 1996] and the terrestrial biosphere [*Siegenthaler and Oeschger*, 1987] to calculate disequilibrium fluxes between atmosphere, ocean, and biosphere.

The dilution of the imprint imposed by adding $^{14}C$-free fossil carbon to the atmosphere (Suess effect) and the redistribution of bomb-produced $^{14}C$ among the carbon reservoirs are governed by the same mechanisms as the dilution of the atmospheric $^{13}C$ perturbation. The atmospheric $^{14}C$ Suess effect and the bomb-produced $^{14}C$ budget are used to test the Bern model and simulated $^{13}C$ disequilibrium fluxes. On the basis of an analysis of the global budget of bomb-produced radiocarbon, *Hesshaimer et al.* [1994] concluded that the oceanic uptake of bomb radiocarbon as reconstructed from oceanic $^{14}C$ measurements has been overestimated by about 20%. Consequently, they postulate that the uptake of anthropogenic $CO_2$ as simulated using models calibrated or validated by the oceanic $^{14}C$ observations has been overestimated by a similar percentage. The budget problem has then been analyzed by other authors as well [*Joos*, 1994; *Broecker and Peng*, 1994; *Broecker et al.*, 1995; *Lassey et al.*, 1996; *Jain et al.*, 1997], who all concluded that the budget is balanced within the uncertainties in the production and in changes of the oceanic, terrestrial, and stratospheric inventories. Here we will analyze the budget of bomb-produced $^{14}C$ in the context of atmospheric and oceanic $^{13}C$ observations and the results of the double deconvolution.

The outline of the paper is as follows. The double deconvolution approach, models, input data, and data treatment are described in the next section. Then, results are presented for the combined ice core and atmospheric records. The budgets and relative importance of different sink terms in the budgets of $^{13}C$ and $^{14}C$ are investigated. Both errors in net carbon fluxes arising from uncertainties in the atmospheric $^{13}C$ and $CO_2$ data as well as uncertainties due to model parameters and the fossil fuel input data are investigated. The main findings and their comparison with results of related studies are presented in the conclusion section.

## 2. Methodology and Input Data

### 2.1. Double Deconvolution Method

The atmospheric $CO_2$ budget is given by

$$\dot{N}_a(t) = F_{\text{fossil}}(t) - F_{\text{as,net}}(t) - F_{\text{ab,net}}(t). \quad (1)$$

The change in atmospheric $CO_2$ $\dot{N}_a(t)$ equals the fossil emissions $F_{\text{fossil}}(t)$ minus the net fluxes into the sea $F_{\text{as,net}}$, and into the biosphere $F_{\text{ab,net}}$. Throughout the text we will use the subscripts a, b, and s to refer to the atmosphere, the biosphere, and the sea (ocean), respectively. The net fluxes are the sum of all gross fluxes into the biosphere and ocean $F_{\text{ab,i}}(t)$ and $F_{\text{as,j}}(t)$ minus the gross fluxes from the biosphere and ocean $F_{\text{ba,i}}(t)$ and $F_{\text{sa,j}}(t)$. Here the subscripts i and j represent different biospheric and surface ocean reservoirs as resolved in a carbon cycle model (Figure 1), i.e.,

$$F_{\text{as,net}}(t) = \sum_j [F_{\text{as,j}}(t) - F_{\text{sa,j}}(t)] \quad (2)$$

$$F_{\text{ab,net}}(t) = \sum_i [F_{\text{ab,i}}(t) - F_{\text{ba,i}}(t)]. \quad (3)$$

As for carbon (equation (1)), we formulate a budget for atmospheric $^{13}CO_2$ as

$$^{13}\dot{N}_a(t) = {}^{13}F_{\text{fossil}}(t) - {}^{13}F_{\text{as,net}}(t) - {}^{13}F_{\text{ab,net}}(t). \quad (4)$$

The net fluxes of $^{13}C$ entering the ocean, $^{13}F_{\text{as,j,net}}$, and the terrestrial biosphere, $^{13}F_{\text{ab,i,net}}$, are expressed with the help of isotopic fractionation factors, $\alpha$, and isotopic ratios, $R$ ($^{13}C/^{12}C$),

$$^{13}F_{\text{as,j,net}}(t) = F_{\text{as,j}}(t)\alpha_{\text{as,j}}R_a(t) - F_{\text{sa,j}}(t)\alpha_{\text{sa,j}}R_{\text{s,j}}(t) \quad (5)$$

$$^{13}F_{\text{ab,i,net}}(t) = F_{\text{ab,i}}(t)\alpha_{\text{ab,i}}R_a(t) - F_{\text{ba,i}}(t)\alpha_{\text{ba,i}}R_{\text{b,i}}(t). \quad (6)$$

Next, we assume that the net carbon flux into the ocean ($F_{\text{as,net}}$) is partitioned between the different surface boxes according to their percentage contribution

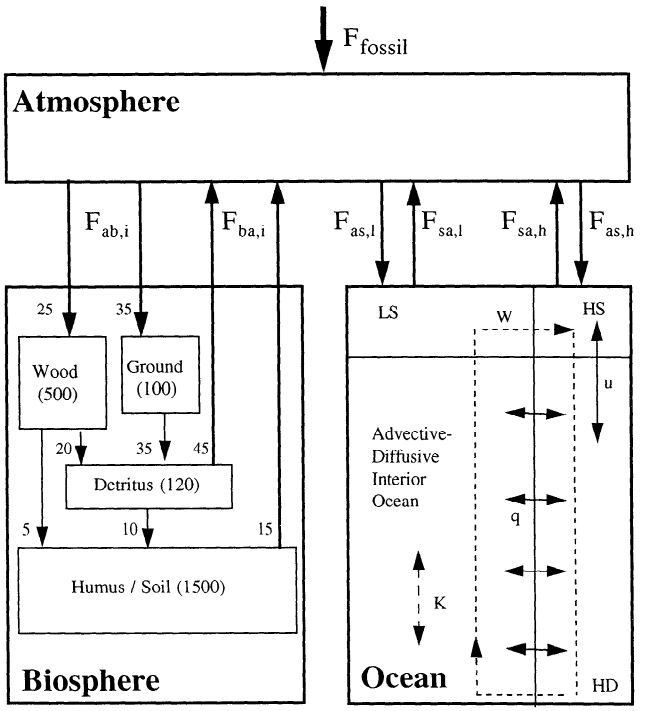


**Figure 1.** Schematic diagram of the Bern model and the carbon fluxes involved in the double deconvolution technique. In the Bern model a well-mixed atmosphere is coupled to the High-Latitude Exchange / Interior Diffusion-Advection (HILDA) ocean model [*Shaffer and Sarmiento*, 1995; *Siegenthaler and Joos*, 1992] and a box model of the terrestrial biosphere [*Siegenthaler and Oeschger*, 1987]. The thick solid arrows describe the fossil emission fluxes ($F_{\text{fossil}}$), gross carbon exchange fluxes between the atmosphere and the surface ocean ($F_{\text{as,j}}$,$F_{\text{sa,j}}$), and the atmosphere and the biosphere ($F_{\text{ab,i}}$, $F_{\text{ba,i}}$) as used in the budget equations for atmospheric $CO_2$ and $^{13}C$ (equations 1 and 10). The HILDA model includes two well-mixed surface boxes, representing low- (LS) and high-latitude surface water masses (HS), a well-mixed high-latitude deep water box (HD), and a diffusive interior reservoir. The eddy diffusivity ($K$) in the interior reservoir is described as a function of depth. Ventilation of the interior ocean by high-latitude waters is described by the parameter $q$, mixing between the two high-latitude boxes is described by the parameter $u$, and advective overturning is described by $w$ (Table 1). The biosphere model includes four reservoirs representing short-lived vegetation and leaves (ground, turnover time $\tau$= 2.9 years), wood ($\tau$= 20 years), detritus($\tau$= 2.2 years), and soil organic carbon ($\tau$= 100 years). Preindustrial carbon fluxes between reservoirs are indicated in units of Gt C yr$^{-1}$. Number in brackets give the preindustrial reservoir size in Gt C.

$p_{\text{s,j}}$ to the total ocean area. Similarly, the net flux into the biosphere ($F_{\text{ab,net}}$) is partitioned between biospheric reservoirs according to the fraction, $p_{\text{b,i}}$, of the total preindustrial carbon input flux obtained by reservoir i,

$$p_{\text{b,i}} = \frac{F_{\text{ab,i}}(t_0)}{\sum_i F_{\text{ab,i}}(t_0)}, \tag{7}$$

where time $t_0$ refers to the preindustrial equilibrium. Where exactly the net biospheric carbon flux $F_{\text{ab,net}}$ is allocated is not relevant for the calculation of the sinks, but a specification is needed to close the model. Subscripts s and b are again added to the percentage factors $p$ to refer to the ocean and the biosphere, respectively; indices i and j again refer to individual biospheric and oceanic reservoirs. Air-to-sea ($F_{\text{as,j}}$) and air-to-biosphere ($F_{\text{ab,i}}$) carbon gross fluxes in (5) and (6) are replaced by

$$F_{\text{as,j}}(t) = F_{\text{sa,j}}(t) + p_{\text{s,j}} F_{\text{as,net}}(t) \tag{8}$$

$$F_{\text{ab,i}}(t) = F_{\text{ba,i}}(t) + p_{\text{b,i}} F_{\text{ab,net}}(t). \tag{9}$$

Then, the $^{13}CO_2$ budget (equation (4)) is reformulated with the help of (5)-(9) by distinguishing terms involving net carbon fluxes ($F_{\text{as,net}}$, $F_{\text{ab,net}}$) and gross carbon fluxes into the atmosphere ($F_{\text{sa,j}}$, $F_{\text{ba,i}}$),

$$\begin{aligned} {}^{13}\dot{N}_{\text{a}}(t) = {} & F_{\text{fossil}}(t) R_{\text{fossil}}(t) \\ & - F_{\text{as,net}}(t) \sum_j p_{\text{s,j}} \alpha_{\text{as,j}} R_{\text{a}}(t) \\ & - F_{\text{ab,net}}(t) \sum_i p_{\text{b,i}} \alpha_{\text{ab,i}} R_{\text{a}}(t) \\ & - \sum_j F_{\text{sa,j}}(t) \left[\alpha_{\text{as,j}} R_{\text{a}}(t) - \alpha_{\text{sa,j}} R_{\text{s,j}}(t)\right] \\ & - \sum_i F_{\text{ba,i}}(t) \left[\alpha_{\text{ab,i}} R_{\text{a}}(t) - \alpha_{\text{ba,i}} R_{\text{b,i}}(t)\right]. \end{aligned} \tag{10}$$

The gross carbon fluxes between sea and air $F_{\text{sa,j}}$, and biosphere and air $F_{\text{ba,i}}$ are multiplied by the isotopic disequilibrium between atmosphere and sea and atmosphere and biota, respectively. Thus we call the last two terms in the $^{13}C$ budget equations the sea-to-air and biota-to-air disequilibrium flux. Note that these definitions will be used in the following when referring to disequilibrium fluxes.

The two budget equations (1) and (10) were solved for the two unknown net air-sea, $F_{\text{as,net}}$, and net air-biota, $F_{\text{ab,net}}$, fluxes at each time step. This requires that all other variables in (1) and (10) be specified.

First, the change in atmospheric inventory of $CO_2$, $\dot{N}_{\text{a}}$, and $^{13}C$, $^{13}\dot{N}_{\text{a}}$, as well as the atmospheric isotopic $^{13}C/^{12}C$ ratio $R_{\text{a}}$ are prescribed by observations. The fossil emission flux $F_{\text{fossil}}$ and its isotopic signature $R_{\text{fossil}}$ are prescribed according to *Marland et al.* [1995] and *Andres et al.* [1996].

Second, the fractionation factors $\alpha_{\text{as,j}}$ and $\alpha_{\text{sa,j}}$ for air-sea exchange fluxes are calculated after *Siegenthaler and Münnich* [1981] and *Mook* [1986] as a function of sea surface temperature. Isotopic fractionation during photosynthesis is about 3 times larger for terrestrial plants

following the C3 photosynthesis pathway than for those following the C4 pathway. We assume that changes in terrestrial carbon storage are related to C3 plants and related soils only [*Keeling et al.*, 1989a; *Quay et al.*, 1992; *Tans et al.*, 1993; *Enting et al.*, 1995; *Francey et al.*, 1995]. This is justified as long as results are not sensitive to C4 plant productivity and if disequilibrium fluxes via the C4 pathway are small. On the other hand, potential long-term trends in the carbon inventory produced by the C4 pathway may alter calculated oceanic and biospheric carbon storage. A release of such C4 carbon into the atmosphere will be partly attributed to a release of oceanic carbon as the isotopic signature of C4 material is heavier than that of C3 carbon. The sensitivity of the calculated net fluxes on the fractionation factor will be tested. No fractionation is assumed for the respiration of biospheric carbon.

Finally, the disequilibrium fluxes (last two lines in (10)) were calculated using the Bern carbon cycle model (Figure 1), which consists of the High-Latitude Exchange / Interior Diffusion-Advection (HILDA) ocean model [*Joos et al.*, 1991a, b; *Siegenthaler and Joos*, 1992; *Shaffer and Sarmiento*, 1995] (version K(z)) and a four-box biosphere model [*Siegenthaler and Oeschger*, 1987]. Both the Bern carbon cycle model and its pulse substitute version [*Joos et al.*, 1996; *Joos and Bruno*, 1996] were used. The behavior of a linear model or model component is fully described by its pulse response (Green's) function. In the substitute model, surface-to-deep tracer transport and biospheric carbon overturning are described by using a pulse response function. The nonlinearities in air-sea exchange, the carbon chemistry, and terrestrial primary production are captured by separate equations. Such nonlinear pulse substitute models consist of a few equations only and require only a modest amount of CPU time while still yielding identical results for atmospheric concentrations as the full model. Additionally, the HILDA model was replaced by pulse substitute versions of the box-diffusion model (BD) [*Oeschger et al.*, 1975], the Geophysical Fluid Dynamics Laboratory (GFDL)/Princeton three-dimensional (3-D) model [*Sarmiento et al.*, 1992] and a 2.5-D model [*Stocker et al.*, 1994]. The model parameters are listed in Table 1. They are the same as those of *Joos et al.* [1996] except when mentioned differently in the text.

The biosphere model is used to calculate the gross carbon fluxes from the biosphere to the atmosphere and its isotopic signature. This is done using a standard box model approach. Carbon turnover between individual boxes and the atmosphere is modeled to be proportional to reservoir sizes.

The gross carbon flux from the surface box $j$ to the atmosphere is calculated as

$$F_{\mathrm{sa,j}}(t) = a_{\mathrm{s,j}} k_{\mathrm{g}} p\mathrm{CO}_{2,\mathrm{j}}(t), \qquad (11)$$

where $a_{\mathrm{s,j}}$ is the surface area of box j and $k_{\mathrm{g}}$ denotes the gas exchange coefficient. The partial pressure, $p\mathrm{CO}_{2,\mathrm{j}}$, is calculated as a function of dissolved inorganic carbon, $\Sigma\mathrm{CO}_{2,\mathrm{j}}$, using a carbon chemistry model [*Fink*, 1996]. Analytical relationships between $p\mathrm{CO}_{2,\mathrm{j}}$ and $\Sigma\mathrm{CO}_{2,\mathrm{j}}$ are given elsewhere [*Joos et al.*, 1996]. The changes in surface water $\Sigma\mathrm{CO}_2$ and $\Sigma^{13}\mathrm{CO}_2$ are obtained as differences between net air-to-sea flux (into reservoir j with area fraction $p_{\mathrm{s,j}}$) and removal by ocean transport

$$\frac{d}{dt}\Sigma\mathrm{CO}_{2,\mathrm{j}} = p_{\mathrm{s,j}} F_{\mathrm{net,as}} - \text{transport} \qquad (12)$$

$$\frac{d}{dt}\Sigma^{13}\mathrm{CO}_{2,\mathrm{j}} = {}^{13}F_{\mathrm{net,as,j}} - \text{transport}. \qquad (13)$$

Thus the ocean model is used to calculate dissolved inorganic carbon as well as its isotopic concentration, $\Sigma^{13}\mathrm{CO}_{2,\mathrm{j}}$, in surface water. This is necessary to calculate the $\mathrm{CO}_2$ partial pressure; the isotopic ratio of $\Sigma\mathrm{CO}_2$, $R_{\mathrm{s,j}}$; the gross fluxes from sea to air, $F_{\mathrm{sa,j}}$; and, finally, the sea-to-air $^{13}\mathrm{C}$ disequilibrium flux in (10).

It may be noted that the net air-sea carbon flux is determined by the $^{13}\mathrm{C}$ budget equation (10) and not by the product of the gas exchange coefficient and air-sea partial pressure difference. Thus the difference in air-sea partial pressure combined with the prescribed gas exchange coefficient is not necessarily consistent with the net air-to-sea flux. We investigated this point by considering two additional solutions of the budget equations.

In the first case we reformulated (10) in order to solve for the sea-to-air instead of solving for the air-to-sea net carbon flux, thereby using observed atmospheric $\mathrm{CO}_2$ values instead of modeled ocean surface $p\mathrm{CO}_2$ values to calculate the oceanic disequilibrium flux. We found that the magnitude of the disequilibrium flux as well as the oceanic uptake increased compared to our standard case where modeled surface $p\mathrm{CO}_2$ values and gross carbon fluxes are relatively low. Deviations in net air-to-sea fluxes for the two cases are smaller than 0.03 Gt C yr$^{-1}$ before 1950 and rise up to 0.3 Gt C yr$^{-1}$ in 1990.

In the second case the disequilibrium fluxes were calculated by running the Bern model in the single deconvolution mode using observed atmospheric $\mathrm{CO}_2$ and $^{13}\mathrm{CO}_2$ observations as boundary conditions. The disequilibrium fluxes calculated in this way were then used in the double deconvolution. This yielded lower net air-to-sea fluxes than in the standard case; deviations are in the range 0.01 to $-0.21$ Gt C yr$^{-1}$.

These results indicate that the inconsistency between air-sea partial pressure and the net air-to-sea flux does not lead to significant errors in the calculated net fluxes prior to 1950. After 1950, differences between our standard case and the first and second cases are noticeable. These deviations in the calculated sinks could be removed if the model was tuned to yield on average the same oceanic uptake in the single and dou-

**Table 1.** Model Parameters

| | Value | Unit |
|---|---|---|
| *Air-Sea Gas Transfer Coefficients* | | |
| Box-diffusion model | 0.0626 | mol $m^{-2}$ $ppm^{-1}$ $yr^{-1}$ |
| HILDA model | 0.0539 | mol $m^{-2}$ $ppm^{-1}$ $yr^{-1}$ |
| 2.5-D model | 0.0655 | mol $m^{-2}$ $ppm^{-1}$ $yr^{-1}$ |
| GFDL/Princeton 3-D model | 0.0638 | mol $m^{-2}$ $ppm^{-1}$ $yr^{-1}$ |
| *$^{13}C$ Fractionation Factors* | | |
| Air-to-sea flux ($F_{as}$) | | |
| Ocean average (BD, HILDA, 2-D, 3-D) | 1.7944 | ‰ |
| HILDA, high-latitudes | 1.7800 | ‰ |
| HILDA, low-latitudes | 1.8700 | ‰ |
| Sea-to-air flux ($F_{sa}$) | | |
| Ocean average (BD, HILDA, 2-D, 3-D) | 10.3624 | ‰ |
| HILDA, high-latitudes | 9.9800 | ‰ |
| HILDA, low-latitudes | 12.3700 | ‰ |
| Air-to-biota flux ($F_{ab}$) | 18.72 | ‰ |
| Biota-to-air flux ($F_{ba}$) | 0 | ‰ |
| *Transport Parameters of the HILDA Model* | | |
| Background eddy diffusivity ($K_0$) | 465 | $m^2$ $yr^{-1}$ |
| Eddy diffusivity at bottom of mixed layer | 7561 | $m^2$ $yr^{-1}$ |
| Eddy diffusivity at 1000 m | 648 | $m^2$ $yr^{-1}$ |
| High-latitude surface-to-deep exchange ($u$) | 38 | m $yr^{-1}$ |
| Upwelling velocity in interior box ($w$) | 0.44 | m $yr^{-1}$ |
| Inverse of exchange coefficient ($q^{-1}$) between deep ocean reservoirs | 538 | years |

Air-sea gas transfer coefficients of the four ocean models are such that the models roughly reproduce the observed oceanic inventory of bomb-produced radiocarbon at time of the Geochemical Ocean Sections Study (GEOSECS) survey. Isotopic fractionations for air-sea exchange were calculated according to *Mook* [1986] and *Siegenthaler and Münnich* [1981]. Transport equations in the spatially resolved three-dimensional (3-D) and 2.5-D models are determined from first-order physical principles and by tuning the models to observed tracer distributions. The box-diffusion and the High-Latitude Exchange / Interior Diffusion-Advection (HILDA) models are spatially aggregated models. Eddy diffusivity in the box-diffusion model is set to 7100 $m^2$ $yr^{-1}$ in order to match the observed penetration of bomb-produced radiocarbon. The transport parameters of the HILDA model (Figure 1) were determined by fitting the model to both the observed distribution of natural and bomb-produced radiocarbon. The eddy diffusivity in the interior reservoir is described as a function of depth $z$ below the bottom of the mixed layer ($K(z)$= [465 + 7096 exp(-$z$/253 m)] $m^2$ $yr^{-1}$). It has been found that such a diffusivity parameterization of the surface-to-deep transport is justified by analyzing results of the Geophysical Fluid Dynamics Laboratory (GFDL)/Princeton 3-D model [*Joos et al.*, 1997].

ble deconvolution simulations. However, we decided to use model parameters (Table 1) determined by fitting the model to the observed oceanic distribution of natural and bomb-produced radiocarbon [*Siegenthaler and Joos*, 1992] and to accept the inconsistency between single and double deconvolution approach in our standard simulations. The main reason is that the atmospheric $\delta^{13}C$ trend cannot be reliably established for the last four decades as will be discussed in the following section on atmospheric data. Thus a redetermination of model parameters appears as premature.

Changes in the carbon fluxes related to the weathering and sedimentation cycles, river fluxes, and the dilution of the atmospheric $\delta^{13}C$ signal by these fluxes were neglected in the two budget equations (1) and (10) and in the model. This is justified as the air-sea and air-biota gross fluxes are 2 orders of magnitude larger. The fluxes $F_{ab,net}$ and $F_{as,net}$ correspond then to oceanic and biospheric carbon storage. One needs to add the preindustrial net fluxes as driven by the weathering/sedimentation cycle to compare the double deconvolution fluxes with estimates of net air-sea and air-

biota fluxes based on observations (see e.g., *Sarmiento and Sundquist* [1992] and *Heimann and Maier-Reimer* [1996] for a discussion). The dilution of the marine surface $\delta^{13}C$ Suess signal by marine biological productivity is neglected as well. A more fundamental assumption is that changes in the isotopic ratio of surface water $\Sigma CO_2$ are mediated by the anthropogenic $CO_2$ transient only. Thus natural fluctuations in the isotopic composition of $\Sigma CO_2$ are neglected.

### 2.2. Atmospheric $CO_2$ and $^{13}C$ Data

Continuous $CO_2$ and $^{13}CO_2$ records are necessary as boundary conditions for the carbon cycle model and to derive the atmospheric growth rates and the atmospheric $^{13}C/^{12}C$ ratio. Data from the three Antarctic cores DE08, DE08-2, and DSS [*Etheridge et al.*, 1996] and direct atmospheric measurements from Mauna Loa and south pole [*Keeling and Whorf*, 1994] were used to reconstruct the history of atmospheric $CO_2$ from the year 1006 to 1992. Monthly, seasonally adjusted Mauna Loa and south pole data were averaged to yield a global mean record. Multiple ice core measurements at the same time were averaged. Then, the discrete ice core data and atmospheric mean values were combined and spline fitted [*Enting*, 1987] to obtain a continuous record. No corrections were applied to merge the two data sets (Figure 2a). For $^{13}C$, data from the Antarctic core Siple [*Friedli et al.*, 1986] and the Arctic core Dye 3 [*Leuenberger*, 1992] were combined with a clean air average of direct atmospheric measurements around 1956 [*Keeling et al.*, 1979] and measurements from Cape Grim [*Francey et al.*, 1996]. The published Siple measurements have been corrected by $-0.1‰$ in order to account for gravitational separation of $^{12}C$ and $^{13}C$ in the firn layer and for an extraction effect [*Leuenberger et al.*, 1992]. These data were spline fitted to form a continuous atmospheric $^{13}C$ record from the year 1744 to 1993 (Figure 2b). The spline fit method described by *Enting* [1987] acts as a low-pass filter. Parameters were selected to obtain approximate cutoff periods of 50 years prior to 1950 and of 10 years for the period of direct atmospheric measurements. The 50 year cutoff for the ice core data period is motivated by the scarcity and quality of the Siple and Dye 3 $^{13}C$ data. It is important to note that between 1956 and 1982 no $\delta^{13}C$ measurements are available. Thus results for this period are unreliable. Model runs were started in 1744 A.D. at the beginning of the $^{13}C$ ice core record.

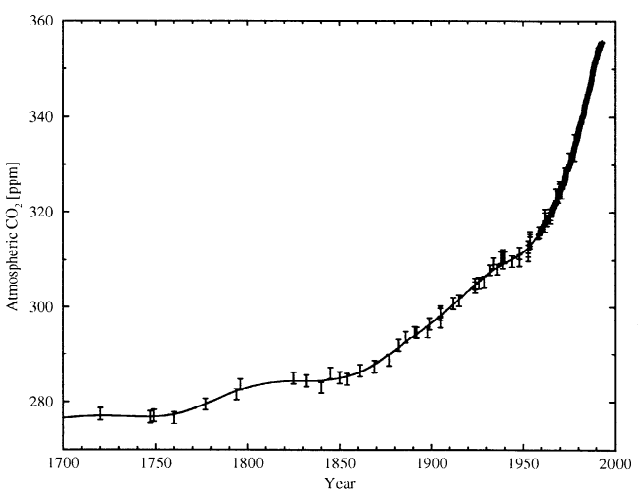


**Figure 2a.** Atmospheric $CO_2$ history. Spline fit (solid curve) through the Law Dome ice core data [*Etheridge et al.*, 1996] and direct atmospheric measurements of $CO_2$ starting in 1958 [*Keeling and Whorf*, 1994]. Data points and 1-$\sigma$ uncertainties of the ice core data ($\pm 1.2$ ppmv) and of the deseasonalized monthly averaged $CO_2$ values from Mauna Loa and south pole (0.1 ppmv) are indicated by error bars. The spline-fitting technique used is that of *Enting* [1987]. Approximate cutoff periods of 50 years for the ice core data and of about 10 years for the atmospheric data were applied; thus frequencies with shorter periods than the cutoff period were attenuated by 50% or more.

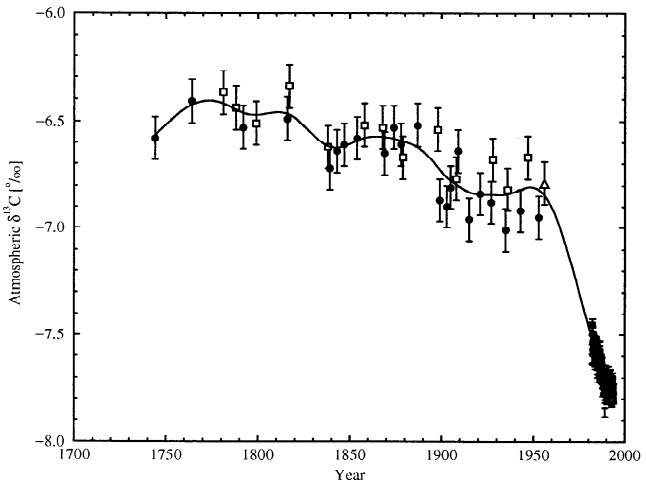


**Figure 2b.** Atmospheric $\delta^{13}C$ history. Spline fit (curve) through the Siple (solid circles) [*Friedli et al.*, 1986], Dye 3 (open squares) [*Leuenberger*, 1992] ice core data, and direct atmospheric measurements around 1956 (open triangle) [*Keeling et al.*, 1979] and at Cape Grim starting in 1982 [*Francey et al.*, 1996]. Cutoff periods are as in Figure 2a.

The direct atmospheric $CO_2$ and $^{13}C$ observations have been smoothed using a cutoff period that is several times longer than the timescale of mixing northern and southern hemisphere air. This is done to avoid the following two problems. First, interannual variations in C4 plant productivity are relatively large. This has the potential to affect calculated terrestrial and oceanic sink fluxes on an interannual timescale as the $^{13}C$ discrimination of C4 plants is substantially lower than that of C3 plants. Second, direct atmospheric measurements from different locations (Cape Grim for $^{13}C$, Mauna

Loa and south pole for $CO_2$) are used to reconstruct the global atmospheric $CO_2$ and $^{13}C$ history. The local trends obtained from these data are then combined with the global fossil emission data. Concentration trends that are of local origin would be misinterpreted as global interannual variations in carbon sources and sinks.

### 2.3. Single Deconvolution and Radiocarbon Simulations

For comparison, the atmospheric $CO_2$ record (cutoff periods of 50 and 10 years) has also been deconvolved by the classical single deconvolution method. Ocean uptake was calculated by the HILDA model, and the biospheric carbon storage ($F_{ab,net}$) is calculated by difference using (1).

Radiocarbon simulations were performed by prescribing the input of $^{14}C$-free fossil fuel and the observed $CO_2$ history in the Bern model to calculate the atmospheric decrease in $\Delta^{14}C$ until 1950. After 1950, atmospheric $\Delta^{14}C$ was prescribed according to observations [*Stuiver and Quay*, 1981; *Nydal and Lovseth*, 1983; *Broecker and Peng*, 1993] as compiled by *Enting et al.* [1994]. All radiocarbon results were obtained by using the single deconvolution methodology to close the atmospheric $CO_2$ budget.

## 3. Results

### 3.1. Oceanic and Biospheric Carbon Storage

A remarkable finding of the double deconvolution is that the trend in biospheric carbon storage between 1900 and today is similar to the trend of the single deconvolution approach (Figure 3a). The single deconvolution yields a large and sudden breakdown in the biospheric source at around 1930. On a 20 year average basis the magnitude of the biospheric source changed by about 0.8 Gt C $yr^{-1}$ from a level of 0.5 to -0.3 Gt C $yr^{-1}$ (sink) [*Bruno and Joos*, 1997]. This change is also present in the double deconvolution results; the magnitude of the biospheric source changed from a level of 0.5 Gt C $yr^{-1}$ to values around -1 Gt C $yr^{-1}$. This sink varies between 0.6 and 2.1 Gt C $yr^{-1}$ for the 1940-1990 period.

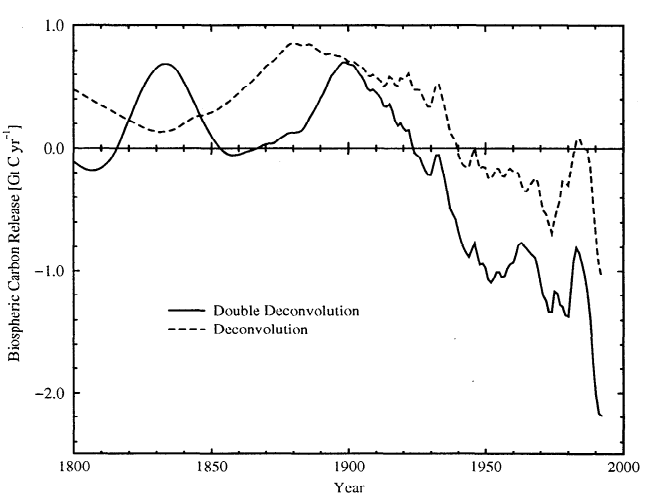


**Figure 3a.** Biospheric carbon release obtained by a double deconvolution of atmospheric $CO_2$ and $^{13}CO_2$ (solid curve) using the Bern carbon cycle model. Also shown is the biospheric carbon release calculated with the single deconvolution method (dashed curve).

Cumulative biospheric carbon released between 1800 and 1950 is estimated to be 64 Gt C in the single deconvolution and 18 Gt C in the double deconvolution approach (Table 2). Between 1950 and 1990, biospheric carbon uptake is estimated to be between 11 (single deconvolution) and 43 Gt C (double deconvolution). Recall, however, that between 1956 and 1982, no isotopic data are available and the atmospheric data point at 1956 is not well connected to modern data. Results of the double deconvolution need therefore to be considered as preliminary and are not very reliable for these decades. This is also true for the most recent years because the calculation depends on the overall history of atmospheric $\delta^{13}C$.

The oceanic storage is considerably larger for the single deconvolution approach, and its evolution is much smoother (Figure 3b). The double deconvolution yielded substantial anticorrelated fluctuations in the ocean and terrestrial uptake. The ocean is even releasing carbon to the atmosphere between 1850 and 1878. We do not consider this release nor the large fluctuations as realistic but as an artifact induced by the relatively large uncertainty of the $^{13}C$ data. Estimated oceanic carbon uptake at 1990 is about 1 Gt C $yr^{-1}$ (double deconvolution) as compared to 2 Gt C $yr^{-1}$ (single deconvolution). Cumulative ocean uptake is almost 3 times as large for the single deconvolution method as for the double deconvolution.

A detailed error analysis for the single deconvolution has been presented earlier by *Bruno and Joos* [1997]. The 1-$\sigma$ error for biospheric carbon storage was estimated to be about 0.2 Gt C $yr^{-1}$ (on a 20 year average basis) for the 1800-1950 period and about 0.5 Gt C $yr^{-1}$ during the last decade. Uncertainties for the double deconvolution are larger and will be presented in section 4. First, the budgets of the carbon isotopes will be examined to study the importance of modeled disequilibrium fluxes and to test the Bern model.

### 3.2. Atmospheric Budget of $^{13}C$

The budget of atmospheric $^{13}C$ as given in (10) is numerically evaluated. Between 1970 and 1990, 0.056 Gt $^{13}C$ $yr^{-1}$ were on average emitted by fossil fuel use. The average atmospheric increase was 0.033 Gt $^{13}C$ $yr^{-1}$. This corresponds to an airborne fraction of

**Table 2.** Comparison of the Results From a Single and Double Deconvolution

| Period | Biospheric Carbon Release, Gt C yr$^{-1}$ | | Oceanic Carbon Uptake, Gt C yr$^{-1}$ | |
|---|---|---|---|---|
| | Single Deconvolution | Double Deconvolution | Single Deconvolution | Double Deconvolution |
| | | *1800-1990: 50 Year Intervals* | | |
| 1800-1850 | 0.256 | 0.253 | 0.172 | 0.169 |
| 1850-1900 | 0.652 | 0.173 | 0.371 | −0.108 |
| 1900-1950 | 0.369 | −0.061 | 0.722 | 0.293 |
| 1950-1990 | −0.266 | −1.077 | 1.413 | 0.603 |
| | | *Whole Period* | | |
| 1800-1990 | 0.280 | −0.131 | 0.630 | 0.220 |

Results are obtained by using the Bern model and prescribed atmospheric $CO_2$ and $^{13}CO_2$ history. The atmospheric $CO_2$ history was reconstructed using the Law Dome ice core data from *Etheridge et al.* [1996] and atmospheric measurements at Mauna Loa and the south pole from *Keeling and Whorf* [1994] (see Figure 2a). The atmospheric $^{13}CO_2$ history was reconstructed from the Antarctic ice core Siple [*Friedli et al.*, 1986] and the Arctic ice core Dye-3 [*Leuenberger*, 1992] in combination with direct atmospheric measurements around 1956 [*Keeling et al.*, 1979] and from Cape Grim [*Francey et al.*, 1996] (see Figure 2b). Cutoff periods of 50 and 10 years were applied for the ice core and atmospheric data, respectively.

59% when defining the fraction as the atmospheric increase divided by the fossil emission. The rest entered the ocean (0.010 Gt $^{13}$C yr$^{-1}$) and the biosphere (0.013 Gt $^{13}$C yr$^{-1}$ ). The disequilibrium fluxes added only a marginal amount of 0.00044 (ocean) and 0.00025 Gt $^{13}$C yr$^{-1}$ (biosphere) to the atmosphere. This corresponds to 1% of the fossil $^{13}$C emission.

Why are the disequilibrium fluxes important although they are so small? The budget equation of $^{13}$C is almost linearly related to that of anthropogenic $CO_2$. The reason is that the $^{13}C/^{12}C$ of different reservoirs and fluxes deviates by only a few per mill from a standard ratio.

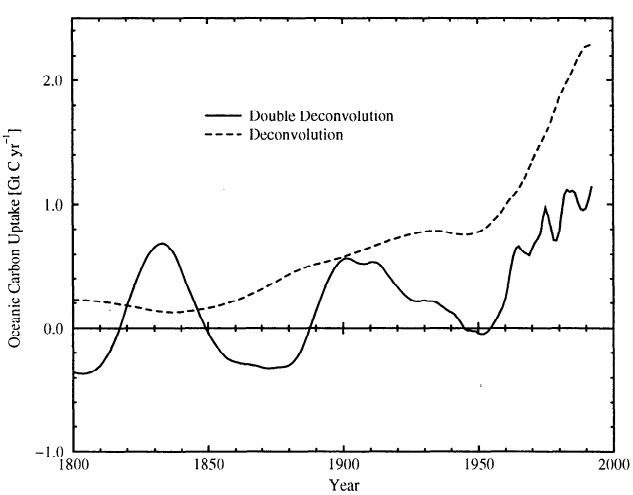


**Figure 3b.** Oceanic carbon uptake obtained by a double deconvolution of atmospheric $CO_2$ and $^{13}CO_2$ (solid curve) using the Bern carbon cycle model. When deconvolving atmospheric $CO_2$, the oceanic carbon uptake is calculated by the HILDA ocean model (dashed curve).

These small deviations and those induced by the disequilibrium fluxes are crucial. These deviations contain the information that allows one to distinguish between different carbon sources. Usually, the $^{13}$C budget equation as given in (10) is therefore recast to analyze the information of the $^{13}$C budget that is independent of the information of the $CO_2$ budget. The important step in the transformation is that the budget of anthropogenic $CO_2$ is subtracted from that of anthropogenic $^{13}$C, thereby removing the correlation between the $^{13}$C and $CO_2$ budget.

Isotopic ratios, $R$, are usually expressed by the $\delta$ notation, which gives the deviation with respect to a standard, $R_{\mathrm{std}}$, as measured in per mill

$$\delta^{13}\mathrm{C} = \frac{R - R_{\mathrm{std}}}{R_{\mathrm{std}}} 1000‰ . \qquad (14)$$

The $^{13}$C budget (equation (10)) is transformed by expressing isotopic ratios, $R$, in $\delta$ notation and fractionation factors, $\alpha$, [e.g., *Mook*, 1986] using the same per mill units,

$$\alpha = 1 + \frac{\varepsilon}{1000‰} . \qquad (15)$$

Then the the budget equation for carbon (equation (1)) is subtracted to obtain the following approximate budget for atmospheric $\delta^{13}$C:

$$\begin{aligned} \frac{d}{dt}(N_{\mathrm{a}}\delta^{13}\mathrm{C}_{\mathrm{a}}) \approx \\ &+F_{\mathrm{fossil}}\delta^{13}\mathrm{C}_{\mathrm{fossil}} \\ &-F_{\mathrm{as,net}}(\delta^{13}\mathrm{C}_{\mathrm{a}} + \varepsilon_{\mathrm{as}}) \\ &-F_{\mathrm{ab,net}}(\delta^{13}\mathrm{C}_{\mathrm{a}} + \varepsilon_{\mathrm{ab}}) \\ &-F_{\mathrm{sa}}\left[(\delta^{13}\mathrm{C}_{\mathrm{a}} + \varepsilon_{\mathrm{as}}) - (\delta^{13}\mathrm{C}_{\mathrm{s}} + \varepsilon_{\mathrm{sa}})\right] \\ &-F_{\mathrm{ba}}\left[(\delta^{13}\mathrm{C}_{\mathrm{a}} + \varepsilon_{\mathrm{ab}}) - (\delta^{13}\mathrm{C}_{\mathrm{b}} + \varepsilon_{\mathrm{ba}})\right] \qquad (16) \end{aligned}$$

**Table 3a.** Budgets of $\delta^{13}C$ and $\Delta^{14}C$ Obtained With the Bern Model

| Term | | $\delta^{13}C$, 1970-1990. ‰ Gt C yr$^{-1}$ | $\Delta^{14}C$, 1860-1950 ‰ Gt C yr$^{-1}$ |
|---|---|---|---|
| 1 | $F_{\text{fossil}} \cdot \delta C_{\text{fossil}}$ | −143 | −659 |
| 2 | $-N_a \cdot \frac{d}{dt}\delta C_a$ | 22 | 143 |
| 3 | $-\frac{d}{dt}N_a \cdot \delta C_a$ | 21 | 6 |
| 4 | $-F_{as,net} \cdot (\delta C_a + \varepsilon_{as})$ | 9 | 7 |
| 5 | $-F_{sa} \cdot [(\delta C_a + \varepsilon_{as}) - (\delta C_s + \varepsilon_{sa})]$ | 39 | 306 |
| 6 | $-F_{ab,net} \cdot (\delta C_a + \varepsilon_{ab})$ | 30 | −5 |
| 7 | $-F_{ba} \cdot [(\delta C_a + \varepsilon_{ab}) - (\delta C_b + \varepsilon_{ba})]$ | 23 | 205 |
| | Airborne fraction ($\gamma$) | 0.20 | 0.22 |

The contribution to total budget of the fossil production (term 1), the change in atmospheric composition (term 2)+(term 3), the ocean and biospheric uptake as attributed to carbon net fluxes (term 4)+(term 6) and the isotopic disequilibrium fluxes (term 5)+(term 7) are listed separately. The $^{13}C$ budget was calculated by applying the double deconvolution methodology; the $\Delta^{14}C$ budget was calculated by a single deconvolution of atmospheric $CO_2$ and prescribed atmospheric $\Delta^{14}C$. Indices a, s, and b denote the atmosphere, the surface ocean, and the terrestrial biosphere, respectively. $F_{\text{fossil}}$ represents the fossil carbon source. $N_a$ represents the atmospheric carbon content, $F_{ij}$ and $F_{ij,net}$ denote carbon gross fluxes or net fluxes from reservoir i to j, and $\delta C$ refers either to $\delta^{13}C$ or $\Delta^{14}C$; fractionation factors, $\varepsilon_{ij}$, are zero for the budget of the fractionation corrected $\Delta^{14}C$. The airborne fraction is the fraction of the total fossil perturbation in the atmospheric isotopic ratio as expressed in units of per mill, which is still found in the atmosphere. It was calculated as described in the text using (19). The airborne fraction, $\gamma$, can be approximated using the absolute values of the above budget terms. It is roughly term 2 divided by the difference of term 1 and term 3 (e.g., for $\Delta^{14}C$, $\gamma$=143/(659-6)).

Here $^{13}C$ fluxes are expressed as the product of carbon fluxes and its isotopic signature in the $\delta$ notation. The units are then ‰ Gt C yr$^{-1}$ . This budget is now not anymore correlated with that of anthropogenic $CO_2$ and allows one to investigate the importance of the different fluxes and reservoir changes. Again, we call the last two terms in this $\delta^{13}C$ budget isotopic disequilibrium fluxes.

Table 3a shows the atmospheric budget for fossil $\delta^{13}C$ for the 1970-1990 period. The net carbon fluxes contributed 27% to the redistribution of the fossil $\delta^{13}C$ signal and the disequilibrium fluxes contributed 43% during this 20 years. This illustrates that the disequilibrium fluxes are indeed important terms that need to be taken carefully into account when the $^{13}C$ budget is used to determine the oceanic and terrestrial sinks. Disequilibrium fluxes of $^{13}C$ in units of ‰ Gt C yr$^{-1}$ are small prior to 1950 (Figure 4). During recent decades, atmospheric $\delta^{13}C$ decreased more rapidly and disequilibrium fluxes became large. We conclude that uncertainties in model parameters or differences between oceanic and terrestrial models have a small impact on the calculated net fluxes prior to 1950 but are significant for the most recent decades. This conclusion is supported by the sensitivity analysis presented in section 4.

The change in the atmospheric product can be further divided into components of the temporal change in $\delta^{13}C$ and $CO_2$,

$$\frac{d}{dt}(N_a\delta^{13}C_a) = N_a\frac{d}{dt}\delta^{13}C_a + \delta^{13}C\,\frac{d}{dt}N_a. \qquad (17)$$

The two components are of roughly equal size (see Table 3a)

As for fossil carbon and $^{13}C$, we define an airborne fraction for $\delta^{13}C$ to further illustrate the importance of

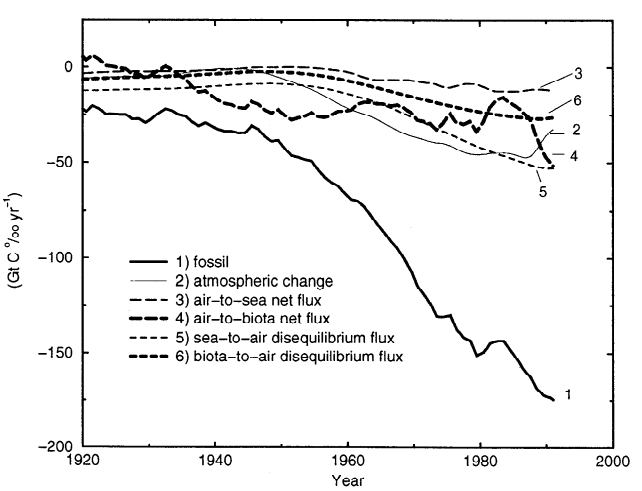


**Figure 4.** The budget of $\delta^{13}C$ as obtained by a double deconvolution of atmospheric $CO_2$ and $^{13}CO_2$ using the Bern model. The individual contribution to the budget is as listed in (16) and described in section 3.2.

the disequilibrium fluxes. First, we calculate the maximal change in the atmospheric signature $d/dt\delta^{13}C_{a,max}$ that would result if the fossil input only affected the atmospheric $\delta^{13}C$ signature and the atmospheric carbon inventory. In such a case the atmospheric change in isotopic composition equals the fossil isotopic input; the change in the atmospheric carbon inventory $d/dtN_a$ equals the fossil input $F_{fossil}$. Using (17) and replacing the change in atmospheric carbon inventory $d/dtN_a$ by the fossil carbon input $F_{fossil}$, one obtains

$$N_a\frac{d}{dt}\delta^{13}C_{a,max} + \delta^{13}C_a F_{fossil} = F_{fossil}\delta^{13}C_{fossil}. \quad (18)$$

Equation (18) is solved for the maximal change of the isotopic signature. The airborne fraction of $\delta^{13}C_a$ is then

$$\gamma = \frac{\frac{d}{dt}\delta^{13}C_a}{\frac{d}{dt}\delta^{13}C_{a,max}} = \frac{N_a\frac{d}{dt}\delta^{13}C_a}{F_{fossil}(\delta^{13}C_{fossil} - \delta^{13}C_a)}. \quad (19)$$

Integration of (19) over time indicates that the airborne fraction of the fossil $\delta^{13}C$ signal is only 20% for the 1970-1990 period. The fraction of the fossil $CO_2$ and $^{13}C$ amount that remained airborne is 3 times larger (59% ) for the same period. Thus a perturbation in the atmospheric $\delta^{13}C$ signature is removed much faster than a perturbation in the atmospheric carbon and $^{13}C$ inventory as noted earlier [*Siegenthaler and Oeschger*, 1987]. This is because the disequilibrium fluxes substantially mute the atmospheric perturbation in the isotopic ratio but not the perturbation in the $^{13}C$ concentration.

The oceanic $^{13}C$ uptake changed the $^{13}C/^{12}C$ of dissolved inorganic carbon. We compare modeled results with observations to test our approach. The Bern model simulates a depth-integrated change of -8.02‰ m yr$^{-1}$ during 1970-1990 as compared to an estimate of -10.4±2.3‰ m yr$^{-1}$ based on observations in the Pacific [*Quay et al.*, 1992].

### 3.3. Atmospheric Budget of $^{14}C$

Atmospheric $\Delta^{14}C$ has decreased by about 20‰ between 1860 and 1950: 17.3‰ are attributed to the input of radiocarbon free fossil fuel (Suess effect), and the remainder is thought to be caused by variation in the cosmic ray production of $^{14}C$ [*Stuiver and Quay*, 1981]. The atomic bomb tests in the late 1950s and early 1960s have added substantial amounts of radiocarbon to the natural background ($^{14}C/^{12}C \approx 10^{-12}$), leading to maximum tropospheric concentrations around 1964. Once test ban treaties were set in place, atmospheric concentration decreased as bomb radiocarbon became absorbed by the biosphere and the biota. Atmospheric explosions were relatively rare after the test ban in 1963, so that the global radiocarbon budget should have remained roughly constant [*Hesshaimer et al.*, 1994].

A similar budget equation as (16) is also applicable for the fossil $\Delta^{14}C$ perturbation when concentrations are expressed in fractionation corrected $\Delta$ units. Table 3a shows the atmospheric $\Delta^{14}C$ budget for the 1860-1950 period (Suess effect). Forty-eight percent of the fossil source entered the ocean, 30% entered the biosphere, and the rest remained airborne (22% ). Almost the entire flux into ocean and biosphere is caused by the disequilibrium fluxes, whereas net carbon fluxes transport only a marginal amount (0.4%) of the $\Delta^{14}C$ signal.

For the bomb budget (Table 3b) the numbers of atoms of $^{14}C$ in different reservoirs are considered. During 1965-1989, 88% of the $^{14}C$ atoms which entered the ocean and 95% which entered the biosphere are attributed to the disequilibrium fluxes in the Bern model. The conclusion is that the $\Delta^{14}C$ Suess effect and the bomb budget provide information on the sum of the disequilibrium fluxes into ocean and biosphere. On the other hand, the budget and the Suess effect do not provide direct information on the net carbon fluxes. Then, the near constancy of the global bomb $^{14}C$ budget [*Hesshaimer et al.*, 1994] as combined with observations of the atmospheric $^{14}C$ decrease and $^{14}C$ production estimates as well as the $\Delta^{14}C$ Suess effect are two additional constraints for modeled disequilibrium fluxes. Another important carbon cycle constraint, the distribution of natural and bomb-produced radiocarbon as observed during the Geochemical Ocean Sections Study (GEOSECS) campaign, has already been used to determine the oceanic mixing parameters and the air-sea gas exchange coefficient of the HILDA ocean model [*Siegenthaler and Joos*, 1992].

In the standard case the bomb-$^{14}C$ budget imbalance is $90\times10^{26}$ atoms between 1965 and 1989 if an atmospheric decrease in $^{14}C$ of $250\times10^{26}$ atoms and a production of $53\times10^{26}$ atoms [*Rath*, 1988; *Hesshaimer et al.*, 1994; *Joos*, 1994] are assumed. The modeled oceanic bomb inventory is $315\times10^{26}$ atoms on January 1, 1975, in agreement with observations. The simulated decrease in atmospheric $\Delta^{14}C$ is 20‰ between 1860 and 1950 if the Bern model is forced by fossil fuel input and observed atmospheric $CO_2$ and $^{13}CO_2$. This is within uncertainty as our ability to reconstruct variability in the cosmic ray production is limited.

In one test of the model the gas exchange coefficient was increased by 46% in order to exactly match the estimated 17.3‰ decrease (1860-1950) in $\Delta^{14}C$ attributed to the fossil signal. The simulated oceanic bomb-radiocarbon inventory in 1974 amounted then to $400\times10^{26}$ atoms, i.e., 30–35% higher than observed [*Broecker et al.*, 1985, 1995]. The modeled budget imbalance increased from $90\times10^{26}$ to $160\times10^{26}$ atoms between 1965 and 1989. In turn, the oceanic carbon storage as modeled by the double deconvolution is increased by 60% and averages 1.6 Gt C yr$^{-1}$ during 1970-1990.

**Table 3b.** Budgets of Bomb-Produced $^{14}C$ Obtained With the Bern model

| | Changes in $^{14}C$ Inventory, $10^{26}$ Atoms | |
|---|---|---|
| | Mid-1965 to Mid-1989 | January 1974 to January 1992 |
| *Changes in Reservoir Size* | | |
| Biosphere | | |
| $-F_{ab,net}(R_a\alpha_{ab})$ | 5 | 1.7 |
| $-F_{ba}(R_a\alpha_{ab} - R_b)$ | 85 | 0.3 |
| Ocean | | |
| $-F_{as,net}(R_a\alpha_{as})$ | 35 | 28 |
| $-F_{sa}(R_a\alpha_{as} - R_s\alpha_{sa})$ | 268 | 107 |
| Troposphere | −145 | −65 |
| Stratosphere | −105 | −34 |
| Total | 143 | 38 |
| *Sources and Sinks* | | |
| Production by nuclear industry | 3 | 3 |
| Radioactive decay | −2 | −2 |
| Production by bomb detonations | 52 | 23 |
| Total | 53 | 24 |
| *Overall Budget* | | |
| Total changes in reservoirs | 143 | 38 |
| Total sources minus sinks | 53 | 24 |
| Imbalance | 90 | 14 |

The decrease in tropospheric $^{14}C$ inventory is derived from atmospheric $CO_2$ and $\Delta^{14}C$ observations. The increase in oceanic and terrestrial storage is calculated by using the Bern model; the isotopic fluxes are attributed to net carbon fluxes and carbon exchange fluxes (disequilibrium fluxes). Bomb test production is estimated based on bomb test statistics [*Hesshaimer et al.*, 1994]. Prior to 1969, the stratospheric decrease is prescribed according to data published by *Tans* [1981] (original measurements corrected downward by 17%). For 1990 an average stratospheric $\Delta^{14}C$ of 200‰ was assumed on the basis of observations above Japan [*Nakamura et al.*, 1992, 1994]. Between 1969 and 1992 these data were exponentially interpolated.

Deviations in net carbon fluxes are smaller than 0.13 Gt C $yr^{-1}$ prior to 1950. For comparison, simulated ocean uptake by the single deconvolution is 1.8 Gt C $yr^{-1}$ for the 1970-1990 period. Hence the carbon sinks calculated by the single and double deconvolution are roughly in agreement. Unfortunately, a large imbalance in the bomb-$^{14}C$ budget is found in this case. More generally, the $^{14}C$ budget imbalance is large when model parameters are changed to yield an ocean uptake as high as that obtained by the single deconvolution.

An improvement of the bomb budget estimates requires that the uptake of radiocarbon by ocean and biosphere be reduced. On the other hand, a reduction in the modeled Suess effect requires an increased radiocarbon uptake by the ocean and biota. This seems hard to achieve, though the timescales involved are different for the two signals. We have tried to match best estimates for the bomb budget and the Suess effect simultaneously by allowing variation in oceanic and biospheric model parameters in a least squares optimization procedure [*Press et al.*, 1989]. Besides the four-box biosphere, a seven-box biosphere was also implemented in order to allow for a wider range of overturning timescales. We could not find improved model solutions. We have also tried to match simultaneously the observed decrease in $\delta^{13}C$ between 1800 and 1990 and to balance the bomb budget using the model in the single deconvolution mode. Again, we could not satisfy the two constraints by applying the same least squares procedure [*Joos et al.*, 1994].

In order to match the best estimate for the bomb-$^{14}C$ budget for the 1965 to 1989 period, the gas exchange coefficient was reduced by a factor of 2. The modeled cumulative budget imbalance between 1965 and 1989 was always less than $13\times10^{26}$ atoms. The simulated oceanic bomb-radiocarbon inventory in 1974 is $176\times10^{26}$ atoms; that is 40% lower than observed. The modeled $\Delta^{14}C$ decrease is 26‰ between 1860 and 1950. The reduced gas exchange leads to smaller disequilibrium fluxes and an unrealistically low oceanic uptake

of 0.1 Gt C $yr^{-1}$ (1970-1990) in the double deconvolution. Also, much lower than observed is the modeled decrease of the $^{13}C/^{12}C$ in dissolved inorganic carbon. This suggests that estimates of bomb test productions and/or the stratospheric $^{14}C$ decrease [*Hesshaimer et al.*, 1994; *Joos*, 1994] are not compatible with $^{13}C$ and $^{14}C$ data.

For the period between GEOSECS and the World Ocean Circulation Experiment (WOCE) (1974-1992) the estimated production and stratospheric decrease are 55 and 67% lower than during the 1965 to 1989 period (Table 3b), and associated errors are reduced. Then, the bomb budget imbalance is reduced to $14\times10^{26}$ in the standard version of the Bern model while simulated oceanic uptake is $135\times10^{26}$ atoms. Eighty percent of the oceanic uptake of bomb-produced $^{14}C$ is attributed to the isotopic disequilibrium flux. The emerging WOCE $^{14}C$ data will therefore allow one to narrow uncertainties of the air-sea gas exchange rate and the disequilibrium fluxes [*Key et al.*, 1996; *Key*, 1996].

## 4. Error Analysis

### 4.1. Uncertainties in the $CO_2$ and $^{13}C$ Data

We performed Monte Carlo simulations to assess the uncertainties in the net fluxes as introduced by uncertainties in the ice core data. Uncertainties of 1-$\sigma$ are 1.2 ppm and 0.1‰ for individual ice core measurements and 0.1 ppm and 0.02‰ for the atmospheric values. The uncertainty in the $\delta^{13}C$ value at 1956 was set to 0.1‰. This is higher than the measurement precision, but the calibration of the mass spectrometer used by *Keeling et al.* [1979] cannot be easily related anymore to modern data. As $\delta^{13}C$ data are missing between 1956 and 1982, results are presented for the period prior to 1950 only. The Monte Carlo analysis was done as described by *Bruno and Joos* [1997]. 2000 runs using Monte Carlo statistics were performed to investigate the link between uncertainties in the atmospheric $CO_2$ and $^{13}CO_2$ history and calculated biospheric (Figure 5) and oceanic carbon storage. One may note that uncertainties are the same for oceanic and biospheric storage. We found for the 1800-1950 period a maximum 1-$\sigma$ uncertainty in the terrestrial and oceanic sink of $\pm0.36$ Gt C $yr^{-1}$. This is considerable as the data have already been smoothed applying a 50 year cutoff period. Estimated overall uncertainty in the net biota uptake for the single deconvolution approach (including uncertainties in ocean model and fossil emissions) are around 0.2 Gt C $yr^{-1}$ for the same period. Thus a substantial fraction of the difference between single and double deconvolution results can be explained by uncertainties in the atmospheric $^{13}CO_2$ (and $CO_2$) data.

For the most recent decades we estimated a 1-$\sigma$ error in the trend of atmospheric $\delta^{13}C$ of approximately $\pm0.01$ ‰ $yr^{-1}$, which yielded an uncertainty in the sinks' distribution of $\pm0.4$ Gt C $yr^{-1}$. One may recall that no $\delta^{13}C$ data are available for the 1956-1982 period. This may potentially induce a larger error in the sinks than $\pm0.4$ Gt C $yr^{-1}$.

### 4.2. Uncertainties in Fossil Emissions

Fossil emissions have a similar isotopic signature as carbon of the terrestrial biosphere. Thus one may view the double deconvolution as a discrimination between oceanic uptake and the sum of the fossil plus the biospheric source. For the fossil fuel data, 1-$\sigma$ uncertainty is estimated to be 10% prior to 1950 and 5% for the most recent decades [*Marland and Rotty*, 1984; *Andres et al.*, 1998; *Keeling*, 1973]. At 1980 this translates into a 1-$\sigma$ uncertainty of $\pm0.30$ Gt C $yr^{-1}$ in net terrestrial carbon storage for an uncertainty in fossil emissions of 0.26 Gt C $yr^{-1}$ when taking into account minor differences in the isotopic signature of fossil and biospheric carbon fluxes.

The isotopic signature of fossil fuel has varied through time. Its $\delta^{13}C$ decreased from $-24$ to $-28.4$‰. Upper error bounds for $\delta^{13}C$ of coal, oil, gas, and cement are viewed to be 0.3, 2.0, 5.0, and 1.0‰, respectively (G. Marland, personal communication, 1996). This yields for the 1980 fuel mix a maximum uncertainty of $\pm1.2$‰ when applying Gaussian error propagation. An uncertainty of $\pm1.0$‰ translates into an error in the terrestrial storage of $\mp0.3$ Gt C $yr^{-1}$ (1980). Following *Heimann and Maier-Reimer* [1996], a 1-$\sigma$ uncertainty of $\pm0.5$‰ is assigned to the fossil $\delta^{13}C$ signature.

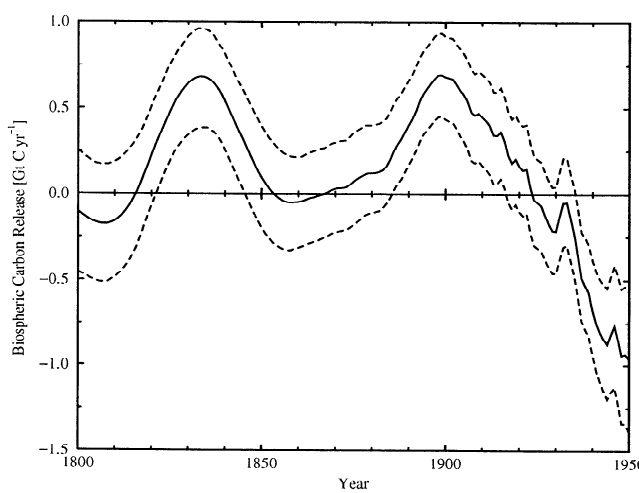


**Figure 5.** Confidence interval of 1-$\sigma$ (dashed curves) of the biospheric carbon release reflecting the influence of the uncertainties in the $CO_2$ and $^{13}CO_2$ data. The 1-$\sigma$ confidence interval is a result of a Monte Carlo analysis including 2000 runs. The best estimate (solid curve) corresponds with the solid curve in Figure 3a.

### 4.3. Uncertainties in Fractionation Factors

Fractionation factors are prescribed as constant in the standard case. Air-sea and sea-air fractionation factors are relatively well known for a given temperature, and related uncertainties in calculated net fluxes are small. However, sea surface temperature and thus fractionation factors have varied with time. In a sensitivity run, fractionation factors were calculated by prescribing the variations of the global mean sea surface temperature according to observations [*Jones*, 1994]. Deviations between the standard case and this sensitivity run are generally small and always less than 0.2 Gt C $yr^{-1}$.

As a standard, we assumed that $C_3$ plants are involved in the biospheric carbon storage process and that the fractionation factor of biospheric carbon is about 18‰ . *Lloyd and Farquhar* [1994] calculated a global average $\delta^{13}C$ discrimination of 14.8‰ when considering both C3 and C4 plants. We employed this value in our model and found deviations in calculated net fluxes up to 0.2 Gt C $yr^{-1}$ prior to 1940 and up to 0.5 Gt C in 1990 (Figure 6). Applying a global mean discrimination factor of 14.8‰ in the four-box biosphere corresponds to an extreme case, as $C_4$ plants contribute predominantly to short-lived material, whereas most of the long-lived material originates from $C_3$ plants.

An open issue is how much the distribution of $C_3$ versus $C_4$ plants and the related terrestrial carbon reservoir have changed over time. Here this question is left to future studies. Similarly, we do not address possible changes in fractionation factors due to changes in land temperature and precipitation. From the above sensitivity studies it is concluded that 1-$\sigma$ uncertainties due to uncertainties in fractionation factors are around 0.1 Gt C $yr^{-1}$ prior to 1950 and may be as large as 0.3 Gt C $yr^{-1}$ in recent decades.

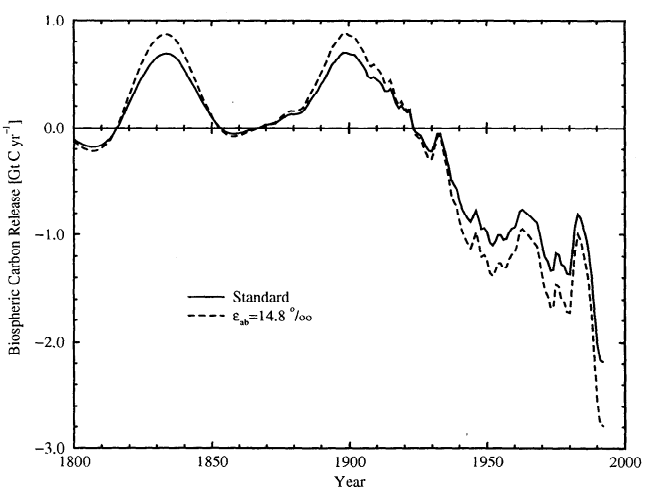


**Figure 6.** Biospheric carbon release obtained by a double deconvolution using the Bern carbon cycle model with a modified biospheric $\delta^{13}C$ discrimination. The fractionation factor of biospheric carbon was set to 14.8‰ following *Lloyd and Farquhar* [1994] (dashed curve) and the result compared with the standard case (solid curve, $\varepsilon_{ab}$=18.72‰ ).

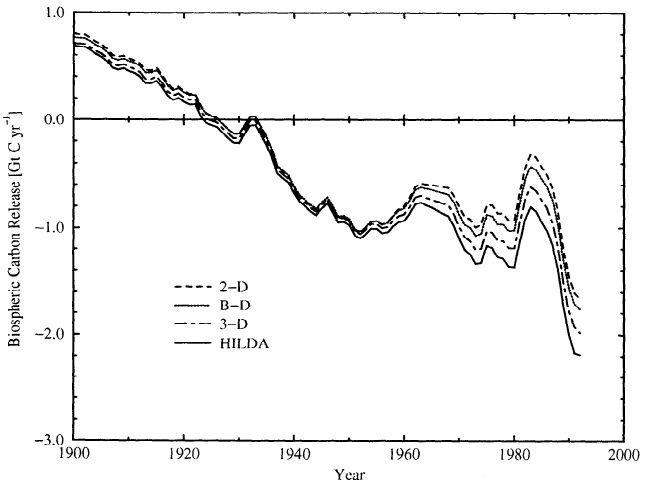


**Figure 7.** Oceanic carbon uptake obtained by a double deconvolution using four ocean models, each combined with the four-box biosphere model: A dynamical two dimensional (2-D) model (dashed curve) [*Stocker et al.*, 1994], the box diffusion model (dotted curve) [*Oeschger et al.*, 1975], the Geophysical Fluid Dynamics Laboratory (GFDL)/Princeton ocean general circulation model (dotted-dashed curve) [*Sarmiento et al.*, 1992], and the HILDA model (solid curve) [*Siegenthaler and Joos*, 1992].

### 4.4. Uncertainties in Modeled Disequilibrium Fluxes

**4.4.1. Results obtained by different ocean models.** The calculation of the disequilibrium fluxes (last two terms in (10)) requires a model. Figure 7 shows the result for the biospheric carbon release for four different ocean models (HILDA, BD, 2-D, and 3-D models) plus the four-box biosphere model. Differences in net fluxes are up to 0.1 Gt C $yr^{-1}$ prior to 1950 and rise then to 0.5 Gt C $yr^{-1}$ in 1990. Next, the air-sea gas exchange rate was set equal in all models. This reduced deviations in net fluxes by a factor of two. The 2-D and the BD models yielded the lowest net air-to-biota fluxes; HILDA yielded a slightly higher biota uptake (0.1 Gt C in 1990), and the 3-D model yielded the largest uptake as it has the least efficient surface-to-deep transport of the models considered here. The deviations in results obtained by the HILDA, the BD, and the 2-D models can be explained almost entirely by different gas exchange coefficients. Here $k_g^{-1}$ is 7.46, 7.66, 7.80, and 9.06 years for the 2-D, 3-D, BD, and HILDA models, respectively. The sensitivity of calculated net fluxes to differences in ocean transport is much smaller than to differences in the gas exchange coefficient (Table 4).

Gas exchange coefficients used in the four ocean models are all based on observations of the oceanic inven-

**Table 4.** Sensitivity Study Regarding a Range of Ocean Models and Model Parameters in the Bern Model

| Model | Disequilibrium Fluxes (1970-1990), Gt C‰ $yr^{-1}$ | | Carbon Sinks (1970-1990), Gt C $yr^{-1}$ | |
|---|---|---|---|---|
| | Sea to Air | Biosphere to Air | Ocean | Biosphere |
| | *Four Ocean Models and Four-Box Biosphere* | | | |
| HILDA | −39.2 | −22.5 | 0.98 | 1.14 |
| 3-D | −40.9 | −22.5 | 1.08 | 1.04 |
| 2-D | −45.9 | −22.4 | 1.37 | 0.75 |
| BD | −44.2 | −22.4 | 1.27 | 0.85 |
| | *Sensitivity Analysis (HILDA and One-Box Biosphere)* | | | |
| Standard | −39.3 | −23.0 | 1.02 | 1.10 |
| $\varepsilon_{ab} \pm 20\%$ | ±0.43 | ±0.12 | ±0.27 | ∓0.27 |
| $k_g \pm 20\%$ | ∓5.53 | ±0.12 | ±0.32 | ∓0.32 |
| $N_b \pm 20\%$ | ±0.14 | ∓2.35 | ±0.13 | ∓0.13 |
| NPP ±20% | ±0.16 | ∓2.55 | ±0.14 | ∓0.14 |

The disequilibrium fluxes and oceanic and biospheric carbon uptake were calculated using the approximate $^{13}CO_2$ budget equation (equation 16, double deconvolution). Results obtained by four different ocean models as applied in their non-linear pulse response representation [*Joos et al.*, 1996] are presented. The atmosphere to biosphere fractionation factor, $\varepsilon_{ab}$; the gas exchange rate, $k_g$; the biospheric mass, $N_b$; and the terrestrial net primary productivity, NPP, have been varied by ±20% around their standard value in HILDA model coupled to a one-box biosphere.

tory in bomb-produced radiocarbon. It is known that the parameterization of the exchange coefficient on wind speeds by *Liss and Merlivat* [1986] leads to a globally averaged gas exchange coefficient for $CO_2$ that is almost 30% smaller than the values inferred from studies of the oceanic uptake of bomb-produced $^{14}C$. The reason of this discrepancy is not clear. However, gas exchange rates for oxygen as inferred from $O_2/N_2$ observations [*Keeling et al.*, 1997] are in general agreement with the bomb-derived $CO_2$ transfer rates. The value used in HILDA (0.054 mol $m^{-2}$ $ppm^{-1}$ $yr^{-1}$) is at the lower end of the range inferred by other authors using radiocarbon data (e.g., 0.063 mol $m^{-2}$ $ppm^{-1}$ $yr^{-1}$ [*Broecker et al.*, 1985], 0.067 mol $m^{-2}$ $ppm^{-1}$ $yr^{-1}$ [*Tans et al.*, 1990], and 0.061 mol $m^{-2}$ $ppm^{-1}$ $yr^{-1}$ [*Wanninkhof*, 1992]) but well within the overall uncertainties of the underlying radiocarbon observations and the functional dependency of the transfer coefficient on wind speed or related quantities.

**4.4.2. Sensitivity analyses.** Individual parameters of the Bern model have been varied while keeping all other parameters fixed. The four-box biosphere has been replaced by a one-box biosphere to reduce the number of parameters. This one-box biosphere (net primary production: 60 Gt C $yr^{-1}$, mass: 1200 Gt C) yielded very similar results as the four-box biosphere; deviations in net fluxes are less than 0.2 Gt C $yr^{-1}$. Varying the air-biota fractionation factor (as expressed in units of per mill), the air-sea gas exchange coefficient, the biomass, and the net primary production by ±20% yielded deviations in the net terrestrial sink as compared to the standard case in the range ±0.31 to ±0.15 Gt C $yr^{-1}$ in 1980 (Table 4). Prior to 1950, deviations are also less than 0.1 Gt C $yr^{-1}$ except for the air-to-biota fractionation factor (deviations less than ±0.33 Gt C $yr^{-1}$). The air-to-biota fractionation factors affect directly the amount of $^{13}C$ transported by the net air-to-biosphere flux $F_{ab,net}$. The disequilibrium flux is hardly affected as the isotopic disequilibrium does not depend on the preindustrial isotopic difference between different reservoirs. Varying all other parameters by ±40% leads to deviations of less than 0.1 Gt C $yr^{-1}$.

Parameters which determine the modeled disequilibrium fluxes most are the air-sea gas exchange coefficient, the primary productivity, and the biospheric overturning time. On the other hand, modeled disequilibrium fluxes are not very sensitive to parameters describing surface-to-deep mixing [*Keeling et al.*, 1989]. This is in contrast to the single deconvolution approach where the oceanic and biospheric sinks are mainly determined by modeled surface-to-deep mixing while the prescribed gas exchange rate is not very relevant. Variations in gas exchange coefficient by ±20% changed modeled $CO_2$ uptake in a single deconvolution by only 0.06 Gt C in 1990. This illustrates that the single and double deconvolution as set up here are independent methods to estimate terrestrial and oceanic carbon storage. On the basis of above results the 1-$\sigma$ error in net fluxes as in-

duced by uncertainties in modeled disequilibrium fluxes is estimated to be around 0.6 Gt C $yr^{-1}$ for the recent decades and 0.2 Gt C $yr^{-1}$ prior to 1950.

### 4.5. Overall Uncertainty in Terrestrial and Oceanic Carbon Storage

Using Gaussian error propagation, a 1-$\sigma$ uncertainty in net oceanic and terrestrial carbon storage of roughly 1 Gt C $yr^{-1}$ is obtained for the most recent decades. Estimated uncertainties due to uncertainties in the $^{13}C$ (and $CO_2$) data ($\pm 0.4$ Gt C $yr^{-1}$), fossil emissions ($\pm 0.3$ Gt C $yr^{-1}$), the fractionation factors ($\pm 0.5$ Gt C $yr^{-1}$), and modeled disequilibrium fluxes ($\pm 0.6$ Gt C $yr^{-1}$) are all relevant. Prior to 1950, overall uncertainty in net fluxes is of similar size but mainly due to the lack of precise $^{13}C$ measurements.

## 5. Discussion and Conclusion

In the double deconvolution the ocean model is not used to calculate net air-sea carbon fluxes; the budget equation for $^{13}CO_2$ provides the necessary information to attribute oceanic and biospheric carbon uptake. Thus the assumption of a steady state natural carbon cycle as used in the single deconvolution can be dropped for the $CO_2$ budget, and it is possible to investigate the long-term variability in the carbon sinks. The single and double deconvolution methods as used here are almost independent, although in both approaches an ocean model is used. Ocean circulation and surface-to-deep mixing is the rate-limiting process for carbon uptake as calculated in the single deconvolution, whereas calculated isotopic disequilibrium fluxes (double deconvolution) depend on the air-sea gas transfer rate but depend only weakly on ocean transport. Results for both methods indicate that the biosphere acted on average as a source during the last century and the first decades of this century in agreement with independent estimates of carbon emissions by land use changes [*Houghton*, 1993]. Then, the biosphere turned into a sink. This implies that a terrestrial sink compensated land use emissions during the last decades. In earlier work we could not attribute this sink to a single mechanism such as $CO_2$ fertilization, nitrogen fertilization, or climate variations [*Bruno and Joos*, 1997].

The double deconvolution technique is similar to the budget method of *Tans et al.* [1993]. *Tans et al.* [1993] use GEOSECS observations of the $^{13}C/^{12}C$ of dissolved inorganic carbon in surface water to estimate the air-sea disequilibrium to be 0.43‰ for the 1970-1990 period. Unfortunately, it is very difficult to accurately determine the global air-sea disequilibrium in $\delta^{13}C$ from oceanic observations; the low average oceanic uptake rate of 0.2 Gt C $yr^{-1}$ during 1970-1990 as calculated by *Tans et al.* [1993] is unrealistically low as it can only account for the increase in surface layer carbon storage. Furthermore, *Tans et al.* [1993] used a constant disequilibrium for the whole 1970-1990 period. In this study, the temporal evolution of the disequilibrium fluxes is modeled by ocean models constrained by radiocarbon observations. This allowed us to calculate temporal variations in the disequilibrium fluxes for the whole industrial period.

Mean oceanic uptake is 0.95 Gt C $yr^{-1}$ during 1982-1992 as found by our double deconvolution. *Francey et al.* [1995] find a mean uptake of about 1.1 Gt C $yr^{-1}$ during the same period. This agreement is to be expected as in both studies, similar techniques and the same $\delta^{13}C$ data are used. On the other hand, *Heimann and Maier-Reimer* [1996] obtained an average ocean uptake of 2.1 Gt C $yr^{-1}$ between 1970 and 1990 based on various $\delta^{13}C$ observations. This is more in line with estimates based on a hierarchy of ocean models that suggest an oceanic uptake rate of 2.0 Gt C $yr^{-1}$ during the 1980-1989 decade [*Orr*, 1993; *Siegenthaler and Sarmiento*, 1993; *Schimel et al.*, 1996].

We have set up the single and double deconvolution as two independent methods to calculate the anthropogenic carbon sinks. Thereby we neglect in the double deconvolution the information about oceanic carbon uptake obtained by analyzing the oceanic distribution of natural and bomb-produced radiocarbon and other transient tracers like CFCs in the framework of the HILDA model [*Joos et al.*, 1991a, b; *Siegenthaler and Joos*, 1992]. In principle, one can combine the two approaches by adjusting model parameters to yield similar results for the oceanic and terrestrial carbon sinks. For example, increasing the air-sea gas exchange coefficient, the air-biota fractionation factor, and net primary productivity by 20% above their standard values yields for both the single and double deconvolution an average oceanic uptake of 1.9 Gt C $yr^{-1}$ during 1970-1990. However, the imbalance in the bomb-$^{14}C$ budget is then even larger as in our standard case. In an earlier study [*Joos et al.*, 1994], we have analyzed most recent but unfortunately still preliminary $^{13}C$ data [*Leuenberger et al.*, 1993]. Oceanic carbon storage was then generally found to be higher for the double deconvolution and more in agreement with estimates based on various ocean models. This suggests that the discrepancy between single and double deconvolution results as found in this study is a consequence of the missing $^{13}C$ data for the 1956-1982 period and is not primarily related to our choice of model parameter values. The mismatch between the two methods will hopefully be resolved in the future when more and more reliable $^{13}C$ data are available.

The Monte Carlo analysis yielded large error bars for the calculated oceanic and terrestrial carbon net fluxes due to uncertainties in the ice core $\delta^{13}C$ data. These error bars have to be viewed in the context of the smoothing applied to the $\delta^{13}C$ data (cutoff period of 50 years).

**Table 5.** Comparison of Carbon Cycle Quantities

| Period | Value | Source |
|---|---|---|
| | *Oceanic Carbon Uptake* | |
| 1970-1990 | 2.1 Gt C $yr^{-1}$ | *Heimann and Maier-Reimer* [1996] |
| | 1.8 Gt C $yr^{-1}$ | *Bruno and Joos* [1997] |
| | 0.91 Gt C $yr^{-1}$ | this study |
| 1982-1992 | 1.1 Gt C $yr^{-1}$ | *Francey et al.* [1995] |
| | 0.95 Gt C $yr^{-1}$ | this study |
| 1980-1989 | 2.0 Gt C $yr^{-1}$ | *Schimel et al.* [1996] |
| | *Biospheric $^{13}C$ Disequilibrium Flux* | |
| 1970-1990 | 23.4 Gt C ‰ $yr^{-1}$ | *Heimann and Maier-Reimer* [1996] |
| | 12.0 Gt C ‰ $yr^{-1}$ | *Quay et al.* [1992], *Tans et al.* [1993] |
| | 22.5 Gt C ‰ $yr^{-1}$ | this study |
| 1987 | 25.8 Gt C ‰ $yr^{-1}$ | *Francey et al.* [1995] |
| | 26.4 Gt C ‰ $yr^{-1}$ | this study |
| 1970-1987 | 17.8 Gt C ‰ $yr^{-1}$ | *Wittenberg and Esser* [1997] |
| | *Oceanic $^{13}C$ Disequilibrium Flux* | |
| 1970-1990 | 50.6 Gt C ‰ $yr^{-1}$ | *Heimann and Maier-Reimer* [1996] |
| | 36.6 Gt C ‰ $yr^{-1}$ | *Tans et al.* [1993] |
| | 39.2 Gt C ‰ $yr^{-1}$ | this study |
| 1987 | 43.8 Gt C ‰ $yr^{-1}$ | *Francey et al.* [1995] |
| | 50.4 Gt C ‰ $yr^{-1}$ | this study |
| | *Air-Sea $^{13}C$ Disequilibrium* | |
| 1970-1990 | 0.43‰ | *Tans et al.* [1993] |
| 1980 | 0.60‰ | this study |
| | *Air-Biota $^{13}C$ Disequilibrium* | |
| 1970-1990 | 0.20‰ | *Tans et al.* [1993] |
| 1980 | 0.38‰ | this study |
| 1988 | 0.33‰ | *Fung et al.* [1997] |
| 1988 | 0.43‰ | this study |
| | *Vertically Integrated Rate of Change of $^{13}C/^{12}C$ in DIC* | |
| 1970-1990 | −10.40‰ m $yr^{-1}$ | *Quay et al.* [1992] |
| | −8.94‰ m $yr^{-1}$ | *Heimann and Maier-Reimer* [1996] |
| | −8.02‰ m $yr^{-1}$ | this study |
| | *Oceanic Bomb $^{14}C$ Inventory* | |
| 1975 | 305× $10^{26}$ atoms | *Broecker et al.* [1995] |
| | 315× $10^{26}$ atoms | this study |
| 1992 | 435× $10^{26}$ atoms | this study |
| | *Bomb $^{14}C$ Budget Imbalance* | |
| 1965-1989 | 82× $10^{26}$ atoms | *Joos* [1994] |
| | 90× $10^{26}$ atoms | this study |
| 1974-1992 | 14× $10^{26}$ atoms | this study |
| | *$\Delta^{14}C$ Suess Effect* | |
| 1860-1950 | 17.3‰ | *Stuiver and Quay* [1981] |
| | 20‰ | this study |

DIC is dissolved inorganic carbon

We conclude that the uncertainty of 0.1‰ in the $\delta^{13}C$ ice core measurements must be reduced to yield more reliable results in a double deconvolution approach. We found a negative correlation between oceanic and biospheric carbon storage on a decadal timescale prior to 1950. We attribute this correlation to the uncertainty in the $^{13}C$ ice core data and do not consider the low oceanic uptake rates as realistic. Note that also *Keeling et al.* [1995] find such a negative correlation on an interannual timescale. These authors interpret the according interannual variations as real and related to El Niño events.

Table 5 summarizes some of the key results of this and related studies. Our disequilibrium fluxes are within the published range. The vertically integrated rate of change of the $^{13}C/^{12}C$ in dissolved inorganic carbon, the oceanic bomb radiocarbon inventory, the global budget of bomb-produced radiocarbon, and the $\Delta^{14}C$ Suess effect are reproduced by the Bern model within the uncertainties of the observations.

The analysis of $\delta^{13}C$ data and the $^{14}C$ Suess effect confirms the high gas exchange rate as derived from the oceanic bomb radiocarbon inventory. Applying a reduced gas exchange yields an unrealistically low oceanic carbon storage for the double deconvolution approach, a too large reduction in $\Delta^{14}C$ prior to 1950, and a too small change of $^{13}C/^{12}C$ in oceanic $\Sigma CO_2$ as compared to observations. Our results suggest that a downward revision of the oceanic bomb inventory as suggested by *Hesshaimer et al.* [1994] is not compatible with the $^{13}C$ data and the $\Delta^{14}C$ Suess constraint. A narrowing of the uncertainties in the bomb budget requires (1) refined estimates of the $^{14}C$ production by weapons test after the atomic bomb test ban treaty has been set in place, and (2) a better quantification of the stratospheric $^{14}C$ history.

Calculated disequilibrium fluxes induce small uncertainties prior to about 1950. For the more recent decades, uncertainties in $^{13}C$ disequilibrium fluxes must be reduced to better quantify the carbon sinks. Emerging radiocarbon data as sampled during the World Ocean Circulation Experiment (WOCE) combined with the GEOSECS results will provide additional information on the oceanic disequilibrium fluxes [*Key et al.*, 1996; *Key*, 1996].

The double deconvolution technique allows one to reconstruct the long-term variability in the carbon cycle. The quality of the reconstruction could substantially be improved if high-precision $\delta^{13}C$ measurements on air entrapped in ice and firn are released, the data gap between 1956 and 1982 is closed, and the temporal trend in atmospheric $\delta^{13}C$ during the last decades is established accurately.

**Acknowledgments.** We thank M. Leuenberger and M. Heimann for valuable suggestions and discussion. M. Leuenberger and R. Francey were helpful in providing their preliminary $\delta^{13}C$ data. Discussions with G. Marland about uncertainties in the fossil fuel isotopic signature are much appreciated. C. Appenzeller, I. Enting, H. Oeschger, J. Sarmiento, T. Stocker, and two unknown reviewers helped to clarify the presentation of the paper. This work was supported by the U.S. Department of Energy (grant DE-FG02-90ER61054), the Swiss National Science Foundation, the Electric Power Research Institute, and the International Atomic Energy Agency (No 8828/CF).

## References

Andres, R. J., G. Marland, and S. Bischoff, Global and latitudinal estimates of $\delta^{13}C$ from fossil-fuel consumption and cement manufacture, *CDIAC Commun., Spring 1996*, 9–10, 1996.

Andres, R. J., G. Marland, T. Boden, and S. Bischoff, Carbon dioxide emissions from fossil fuel combustion and cement manufacture 1751-1991 and an estimate of their isotopic composition and latitudinal distribution, in *The Carbon Cycle*, edited by T. M. L. Wigley and D. Schimel, Cambridge Univ. Press, New York, 1998.

Broecker, W. S., and T.-H. Peng, Evaluation of the $^{13}C$ constraint on the uptake of fossil fuel $CO_2$ by the ocean, *Global Biogeochem. Cycles, 7*(3), 619–626, 1993.

Broecker, W. S., and T.-H. Peng, Stratospheric contribution to the global bomb radiocarbon inventory: Model versus observation, *Global Biogeochem. Cycles, 8*(3), 377–384, 1994.

Broecker, W. S., T. H. Peng, G. Ostlund, and M. Stuiver, The distribution of bomb radiocarbon in the ocean, *J. Geophys. Res., 90*, 6953–6970, 1985.

Broecker, W. S., S. Sutherland, W. Smethie, T.-H. Peng, and G. Ostlund, Oceanic radiocarbon: Separation of the natural and bomb components, *Global Biogeochem. Cycles, 9*(2), 263–288, 1995.

Bruno, M., and F. Joos, Terrestrial carbon storage during the past 200 years: A Monte Carlo analysis of $CO_2$ data from ice core and atmospheric measurements, *Global Biogeochem. Cycles, 11(1)*, 111–124, 1997.

Ciais, P., P. P. Tans, M. Trolier, J. W. C. White, and R. J. Francey, A large northern hemispheric terrestrial $CO_2$ sink indicated by the $^{13}C/^{12}C$ ratio of atmospheric $CO_2$, *Science, 269*, 1098–1102, 1995.

Enting, I. G., On the use of smoothing splines to filter $CO_2$ data, *J. Geophys. Res., 92*, 10977–10984, 1987.

Enting, I. G., T. M. L. Wigley, and M. Heimann, Future emissions and concentrations of carbon dioxide: Key ocean/atmosphere/land analyses, *Techn. Rep. 31, CSIRO*, Div. of Atmos. Res., Melbourne, Victoria, Australia, 1994.

Enting, I. G., C. M. Trudinger, and R. J. Francey, A synthesis inversion of the concentration and $\delta^{13}C$ of atmospheric $CO_2$, *Tellus, Ser. B, 47*, 35–52, 1995.

Etheridge, D. M., L. P. Steele, R. L. Langenfelds, R. J. Francey, J.-M. Barnola, and V. I. Morgan, Natural and anthropogenic changes in atmospheric $CO_2$ over the last 1000 years from air in Antarctic ice and firn, *J. Geophys. Res., 101*, 4115–4128, 1996.

Fink, R., Zur Kohlenstoffchemie des Ozeans und zur Modellierung des natürlichen Kohlenstoffkreislaufes, Ph.D thesis, Univ. Bern, Bern, Switzerland, 1996.

Francey, R. J., P. P. Tans, C. E. Allison, I. G. Enting, J. W. C. White, and M. Troller, Changes in oceanic and terrestrial carbon uptake since 1982, *Nature, 373*, 326–330, 1995.

Francey, R. J., C. E. Allison, E. D. Welch, I. G. Enting, and H. S. Goodman, In situ $\delta^{13}C$ and $\delta^{18}O$ ratios of atmospheric $CO_2$ from Cape Grim, Tasmania, Australia: 1982-1993, *CDIAC Commun., Spring 1996*, 10 11, 1996.

Friedli, H., H. Loetscher, H. Oeschger, U. Siegenthaler, and B. Stauffer, Ice core record of the $^{13}C/^{12}C$ ratio of atmospheric carbon dioxide in the past two centuries, *Nature, 324*, 237–238, 1986.

Fung, I., et al., Carbon 13 exchanges between the atmosphere and biosphere, *Global Biogeochem. Cycles, 11(4)*, 507–533, 1997.

Heimann, M., and E. Maier-Reimer, On the relations between the oceanic uptake of $CO_2$ and its carbon isotopes, *Global Biogeochem. Cycles, 10*(1), 89–110, 1996.

Hesshaimer, V., M. Heimann, and I. Levin, Radiocarbon evidence for a smaller carbon dioxide sink than previously believed, *Nature, 370*, 201–203, 1994.

Houghton, R. A., Changes in terrestrial carbon over the last 135 years, in *The Global Carbon Cycle,* vol. I15, edited by M. Heimann, pp. 139–157, Springer-Verlag, 1993.

Jain, A. K., H. S. Kheshgi, and D. J. Wuebbles, Is there an imbalance in the global budget of bomb-produced radiocarbon?, *J. Geophys. Res., 102*, 1327–1333, 1997.

Jones, P. D., Hemispheric surface air temperature variations: A reanalysis and an update to 1993, *J. Clim., 7*, 1794–1802, 1994.

Joos, F., Imbalance in the budget, *Nature, 370*, 181–182, 1994.

Joos, F., and M. Bruno, Pulse response functions are cost-efficient tools to model the link between carbon emissions, atmospheric $CO_2$ and global warming, *Phys. Chem. Earth, 21*, 471–476, 1996.

Joos, F., J. L. Sarmiento, and U. Siegenthaler, Estimates of the effect of Southern Ocean iron fertilization on atmospheric $CO_2$ concentrations, *Nature, 349*, 772–774, 1991a.

Joos, F., U. Siegenthaler, and J. L. Sarmiento, Possible effects of iron fertilization in the Southern Ocean on atmospheric $CO_2$ concentration, *Global Biogeochem. Cycles, 5*(2), 135–150, 1991b.

Joos, F., M. Bruno, M. Leuenberger, and R. Francey, Carbon isotopes as constraints for global carbon cycle models, in *Final Report: Isotope Variations of Carbon Dioxide and Other Trace Gases in the Atmosphere*, edited by K. Rozanski, pp. 5, Int. At. Energy Agency, Vienna, 1994.

Joos, F., M. Bruno, R. Fink, T. F. Stocker, U. Siegenthaler, C. Le Quéré, and J. L. Sarmiento, An efficient and accurate representation of complex oceanic and biospheric models of anthropogenic carbon uptake, *Tellus, Ser. B, 48*, 397–417, 1996.

Joos, F., J. C. Orr, and U. Siegenthaler, Ocean carbon transport in a box-diffusion versus a general circulation model, *J. Geophys. Res., 102*, 12367–12388, 1997.

Keeling, C. D., Industrial production of carbon dioxide from fossil fuels and limestone, *Tellus, 25*, 174–197, 1973.

Keeling, C. D., and T. P. Whorf, Atmospheric $CO_2$ records from sites in the SIO network, in *Trends '93: A Compendium of Data on Global Change*, edited by T. Boden et al., pp. 16–26, Carbon Dioxide Inf. Anal. Cent., Oak Ridge, Tenn., 1994.

Keeling, C. D., W. G. Mook, and P. Tans, Recent trends in the $^{13}C/^{12}C$ ratio of atmospheric carbon dioxide, *Nature, 277*, 121–123, 1979.

Keeling, C. D., R. B. Bacastow, A. F. Carter, S. C. Piper, T. P. Whorf, M. Heimann, W. G. Mook, and H. Roeloffzen, A three-dimensional model of atmospheric $CO_2$ transport based on observed winds, 1, Analysis of observational data, in *Aspects of Climate Variability in the Pacific and the Western Americas, Geophys. Monogr. Ser.*, vol. 55, edited by D. H. Peterson, pp. 165–236, AGU, Washington, D. C., 1989a.

Keeling, C. D., S. C. Piper, and M. Heimann, A three dimensional model of atmospheric $CO_2$ transport based on observed winds: 4. Mean annual gradients and interannual variations, in *Aspects of Climate Variability in the Pacific and the Western Americas, Geophys. Monogr. Ser.*, vol. 55, edited by D. H. Peterson, pp. 305–363, AGU, Washington, D. C., 1989b.

Keeling, C. D., T. P. Whorf, M. Wahlen, and J. v. d. Pflicht, Interannual extremes in the rate of atmospheric carbon dioxide since 1980, *Nature, 375*, 666–670, 1995.

Keeling, R. F., B. B. Stephens, R. G. Najjar, S. C. D. D. Archer, and M. Heimann, Seasonal variations in the atmospheric $O_2/N_2$ ratio in relation to the kinetics of air-sea gas exchange, in *5th International $CO_2$ Conference, Cairns, 8-12 September 1997, Extended Abstracts*, p. 92, CSIRO Div. of Atmos. Res., Aspendale, Victoria, Australia, 1997.

Key, R. M., WOCE Pacific Ocean radiocarbon program, *Radiocarbon, 38*, 415–423, 1996.

Key, R. M., P. D. Quay, G. A. Jones, A. P. McNichol, K. F. von Reden, and R. J. Schneider, WOCE AMS radiocarbon I: Pacific Ocean results (P6, P16 and P17), *Radiocarbon, 38*, 425–518, 1996.

Lassey, K. R., I. G. Enting, and C. M. Trudinger, The earth's radiocarbon budget: A consistent model of the global carbon and radiocarbon cycles, *Tellus, Ser. B, 48*, 487–501, 1996.

Leuenberger, M., Isotopen- sowie Konzentrationsbestimmungen an $CO_2$, $N_2O$, $O_2$ und $N_2$ in Luftproben aus polarem Eis, Ph.D. thesis, Univ. Bern, Bern, Switzerland, 1992.

Leuenberger, M., U. Siegenthaler, and C. C. Langway, Carbon isotope composition of atmospheric $CO_2$ during the last ice age from an Antarctic ice core, *Nature, 357*, 488–490, 1992.

Leuenberger, M., R. Francey, D. Etheridge, C. Allison, and I. Enting, High precision $\delta^{13}C$ and $CO_2$ concentration measurements from a high time resolution Antarctic ice core, in *Abstracts: 4th International $CO_2$ Conference, Carqueiranne, 13-17 September 1993,* Global Atmos. Watch, Rep. 89, pp. 197–198, World Meteorol. Organ., Geneva, 1993.

Liss, P. S., and L. Merlivat, Air-sea exchange rates: Introduction and synthesis, in *The Role of Air-Sea Exchange in Geochemical Cycling*, edited by Buat-Menard, pp. 113–127, D. Reidel, Norwell, Mass., 1986.

Lloyd, J., and G. D. Farquhar, $^{13}C$ discrimination during $CO_2$ assimilation by the terrestriala biosphere, *Oecologia, 99*, 201–215, 1994.

Marland, G., and R. M. Rotty, Carbon dioxide emissions from fossil fuels: A procedure for estimation and results for 1950-1982, *Tellus, Ser. B, 36*, 232–261, 1984.

Marland, G., T. A. Boden, and R. J. Andres, Global, regional and national annual $CO_2$ emission estimates from fossil-fuel burning, hydraulic-cement production and gas flaring: 1950 to 1992, *CDIAC Commun., Fall 1995*, 20–21, 1995.

Mook, W. G., $^{13}C$ in atmospheric $CO_2$, *Neth. J. Sea Res., 20*(2/3), 211–223, 1986.

Nakamura, T., T. Nakazawa, N. Nakai, H. Kitagawa, H. Honda, T. Itoh, T. Machida, and E. Matsumoto, Measurements of $^{14}C$ concentrations of stratospheric $CO_2$ by accelerator mass spectrometry, *Radiocarbon, 34*, 745–752, 1992.

Nakamura, T., T. Nakazawa, H. Honda, H. Kitaawa, T. Machida, A. Ikeda, and E. Matsumoto, Vertical distributions of $^{14}C$ concentrations for lower stratospheric $CO_2$ measured with accelerator mass spectrometer, in *Proceedings of the International Symposium on Global Cycles of Atmospheric Greenhouse Gases, March 7-10, 1994, Senday, Japan*, pp. 226–234, Tohoku Univ., Sendai, Japan, 1994.

Nydal, R., and K. Lovseth, Tracing bomb $^{14}C$ in the atmosphere 1962-1980, *J. Geophys. Res., 88*, 3621–3642, 1983.

Oeschger, H., U. Siegenthaler, U. Schotterer, and A. Gugelmann, A box diffusion model to study the carbon dioxide exchange in nature, *Tellus, 27*, 168–192, 1975.

Orr, J. C., Accord between ocean models predicting uptake of anthropogenic $CO_2$, *Water Air Soil Pollut., 70*, 465–481, 1993.

Pearman, G. I., and P. Hyson, Global transport and interreservoir exchange of carbon dioxide with particular reference to stable isotope distribution, *J. Atmos. Chem., 4*, 81–124, 1986.

Press, W. H., B. P. Flannery, S. A. Teukolsky, and W. T. Vetterling, *Numerical Recipes*, Cambridge Univ. Press, New York, 1989.

Quay, P. D., B. Tilbrook, and C. S. Wong, Oceanic uptake of fossil fuel $CO_2$: Carbon-13 evidence, *Science, 256*, 74–79, 1992.

Rath, H. K., Ph.D. thesis, Univ. Heidelberg, Heidelberg, Germany, 1988.

Sarmiento, J. L., and E. T. Sundquist, Revised budget for the oceanic uptake of anthropogenic carbon dioxide, *Nature, 356*, 589–593, 1992.

Sarmiento, J. L., J. C. Orr, and U. Siegenthaler, A perturbation simulation of $CO_2$ uptake in an ocean general circulation model, *J. Geophys. Res., 97*, 3621–3645, 1992.

Schimel, D., D. Alves, I. Enting, M. Heimann, F. Joos, D. Raynaud, and T. Wigley, $CO_2$ and the carbon cycle, in *IPCC Second Scientific Assessment of Climate Change*, edited by J. Houghton, pp. 76–86, Cambridge Univ. Press, New York, 1996.

Shaffer, G., and J. Sarmiento, Biogeochemical cycling in the global ocean 1, A new, analytical model with continuous vertical resolution and high-latitude dynamics, *J. Geophys. Res., 100*, 2659–2672, 1995.

Siegenthaler, U., and F. Joos, Use of a simple model for studying oceanic tracer distributions and the global carbon cycle, *Tellus, Ser. B, 44*, 186–207, 1992.

Siegenthaler, U., and K. O. Münnich, $^{13}C/^{12}C$ fractionation during $CO_2$ transfer from air to sea, in *SCOPE*, vol. 16, *Carbon Cycle Modelling*, edited by B. Bolin, pp. 249–257, John Wiley, New York, 1981.

Siegenthaler, U., and H. Oeschger, Biospheric $CO_2$ emissions during the past 200 years reconstructed by deconvolution of ice core data, *Tellus, Ser. B, 39*, 140–154, 1987.

Siegenthaler, U., and J. L. Sarmiento, Atmospheric carbon dioxide and the ocean, *Nature, 365*, 119–125, 1993.

Stocker, T. F., W. S. Broecker, and D. G. Wright, Carbon uptake experiments with a zonally averaged global circulation model, *Tellus, Ser. B, 46*, 103–122, 1994.

Stuiver, M., and P. D. Quay, Atmospheric $^{14}C$ changes resulting from fossil fuel $CO_2$ release and cosmic ray flux variability, *Earth Planet. Sci. Lett., 53*, 349–362, 1981.

Tans, P., A compilation of bomb $^{14}C$ data for use in global carbon model calculation, in *SCOPE*, vol. 16, *Carbon Cycle Modelling*, edited by B. Bolin, pp. 131–137, John Wiley, New York, 1981.

Tans, P. P., I. Y. Fung, and T. Takahashi, Observational constraints on the global atmospheric $CO_2$ budget, *Science, 247*, 1431–1438, 1990.

Tans, P. P., J. A. Berry, and R. F. Keeling, Oceanic $^{12}C/^{13}C$ observations: A new window on ocean $CO_2$ uptake, *Global Biogeochem. Cycles, 7*(2), 353–368, 1993.

Wanninkhof, R., Relationship between wind speed and gas exchange over the ocean, *J. Geophys. Res., 97*, 7373–7382, 1992.

Wittenberg, U., and G. Esser, Evaluation of the isotopic disequilibrium in the terrestrial biosphere by a global carbon isotope model., *Tellus, Ser. B, 49*, 263–269, 1997.

M. Bruno and F. Joos, Physics Institute, University of Bern, Sidlerstr. 5, CH-3012 Bern, Switzerland. (e-mail: mbruno@sairgroup.com; joos@climate.unibe.ch)

(Received August 5, 1997; revised February 2, 1998; accepted February 23, 1998.)